

5 EXPERIMENTAL⁸

5.1 Experimental procedures for Chapter 6

5.1.1 Waxy Oil green coke

Four samples of high-ash Waxy Oil green coke were obtained from the Sasol Synfuels delayed coker at Secunda. The samples were dried and sieved to obtain a particle size fraction of 10–60 mm. This size fraction was crushed to obtain smaller size fractions for analysis, calcination and graphitisation.

5.1.2 Standard analyses

The methods used to characterise the Waxy Oil green coke are shown in Table 5-1.

Table 5-1 Standard test methods used to characterise Waxy Oil green/calcined coke⁹

Analysis	Units	Test method
Ash content	Mass %	ASTM D-4422-89
Volatile Carbon Matter (VCM)	Mass %	BS-1016 Part 4
Carbon	Mass %	LECO CHN Analyzer
Hydrogen	Mass %	LECO CHN Analyzer
Nitrogen	Mass %	LECO CHN Analyzer
Sulphur	Mass %	ASTM D-4239-94
Hardgrove Grindability Index (HGI)		ASTM D-409/D-5003
CO ₂ reactivity	Mass %, 100 min ⁻¹	Alusuisse C110
Vibrated Bulk Density (VBD)	g.cm ⁻³	ASTM D-4992-092
Density (-75 μm; helium)	g.cm ⁻³	ASTM D-5018-89
Metals	Mass %	UOP 927-92

5.1.3 Thermogravimetric Analysis (TGA)

TGA and DTG curves of the Waxy Oil green coke and pre-graphite¹⁰ samples (-150 μm) were obtained using a Mettler TGA1/DSC1 thermogravimetric instrument.

The following programme was used:

- Equilibrate at 30 °C for 3 min under nitrogen flow of 150 ml.min⁻¹
- 30 °C to 110 °C, rate 50 °C.min⁻¹, under nitrogen flow of 150 ml.min⁻¹
- 110 °C for 3 min under nitrogen flow of 150 ml.min⁻¹
- 110 °C to 900 °C, rate 50 °C.min⁻¹, under nitrogen flow of 150 ml.min⁻¹
- 900 °C for 7 min under nitrogen flow of 150 ml.min⁻¹
- 900 °C for 20 min under air flow of 150 ml.min⁻¹

⁸ Unless otherwise stated, all the experimental procedures and analyses were conducted by the author.

⁹ Standard ASTM analyses were conducted by the Sasol Synfuels quality laboratory.

¹⁰ “Pre-graphite” is the term used in this thesis to describe Waxy Oil green coke heat treated to 2 000 °C in an inert atmosphere.

5.1.4 Optical microscopy

Samples of the green and calcined cokes (+20 mm) were mounted in epoxy resin and polished using ISO 7404-2 (1985) as a guideline. The samples were examined under oil immersion using a Leica DM4500P petrographic polarised light microscope.

Optical microscopy was conducted under Bright field conditions. As the simplest of all microscopy techniques, the contrast is caused by the absorbance of white light in accordance with the density of the various parts of the coke sample. The micrographs were conducted using oil immersion with a 50x objective (thus making the magnification 500x) taking into account the 10x magnification of the ocular lens without an optical polarizer. Thus the catalyst appears as a dark brown colour and the carbon microstructure as a light brown colour. As pores absorb all the white light they appear as a black colour. The scale used for the micrographs is 20 microns.

5.1.5 Calcination

5.1.5.1 Calcination process

Waxy Oil green coke (2–10 mm; approximately 350 g) was calcined in a muffle oven with a nitrogen flux using the following temperature programme:

- Ambient (25 °C) to 1 000 °C at approximately 5 °C.min⁻¹; duration 200 min
- 1 000 °C to 1 400 °C at approximately 2 °C.min⁻¹; duration 200 min
- Temperature maintained at 1 400 °C for 80 min
- Cooling to ambient room temperature overnight under nitrogen flux
- The sample was weighed to determine the yield.

5.1.5.2 Standard analyses

The standard analyses are shown in Table 5-1.

5.1.5.3 X-ray Diffraction (XRD)

X-ray powder diffraction data were collected using a Phillips X-pert Pro multi-purpose diffractometer equipped with the X'Celerator detector. The data were acquired at a scanning speed of 0.014 °2θ/s with a step size of 0.017 °2θ and line broadening was conducted. Samples were irradiated with iron-filtered cobalt (Co) K_α X-rays emitted from a sealed tube source. Crystalline phases present in the sample were identified by searching the powder diffraction file database (PDF-4+ 2008) using the X'Pert HighScore Plus Version 2.2d PAN analytical software. The phase's line broadening (from which the L_c values were determined) were obtained by deconvoluting the phase's line broadening from instrumental line broadening – the so-called “fundamental parameters approach” in the software Topas 4.2 in a process of Rietveld refinement. The instrument broadening is determined by measuring a powder diffractogram of a crystalline standard, lanthanum hexaboride (LaB₆).

The powder samples were packed using the back-loading technique to minimise preferred orientation. Each sample was packed and analysed three times to determine the standard deviation.

5.1.5.4 Raman spectroscopy

Samples were placed on a microscope slide and measured using the inVia Raman system, utilising the 514.5 nm line of a 5.3 mW (at the sample) Ar-ion ion laser beam that was focused with a Leica microscope using a x 20 long focus objective. Data were obtained for the region 200–4000 cm^{-1} for 60 s, scanned five times using a laser power of 100% with a 75% defocused beam. Four to five separate spectra were obtained for each sample and then averaged to obtain the final spectrum used for analysis. Wire Version 2, Service Pack 8 software was used for data capturing and instrument control. The Raman band of pure Si was measured before data accumulation commenced for calibration purposes. Normalisation and band deconvolution were done using OPUS software, Version 6, using the Levenberg-Marquardt algorithm. Deconvoluted band shapes were described using pseudo-Voigt functions.

5.1.5.5 Scanning Electron Microscopy (SEM)

Coke samples were stabilised in epoxy resin and polished using ISO 7404-2 (1985) as a guideline. The samples were immersed in ethanol and dried in an oven (at 60 °C). Gold plating was conducted on an Emitech K550X instrument. The SEM photo was obtained on a JEOL JSM-840 Scanning Electron Microscope.

5.1.6 Pre-graphitisation

5.1.6.1 Pre-graphitisation process¹¹

The four high-ash Waxy Oil green cokes were pre-graphitised by the author at the National Energy Corporation of South Africa (NECSA). A medium-frequency induction furnace was used to pre-graphitise the samples. The green coke (approximately 17 g; -2.0 mm) was placed in a cylindrical graphite crucible with a graphite lid. The crucible was wrapped with an inner layer of graphite wool insulator and an outer layer of alumina wool. The insulated sample was wedged in between the copper coil. The reactor was closed and a vacuum pump evacuated the reactor to -0.8 bar. The reactor was then connected to an argon line and the pressure kept constant at -0.6 bar.

The power was set at 6 kW for 5 min up to a temperature of 1 500 °C. It was then increased to 17 kW to attain a maximum temperature (measured with a pyrometer) of approximately 2 000 °C, which was maintained for 5 min. The reactor was cooled for an hour and the sample of pre-graphite was weighed to determine the yield.

5.1.6.2 Standard analyses

The test method used to determine the density of the pre-graphite (-75 μm) is shown in Table 5-1. A particle size of -75 μm was chosen to exclude the greater part of the internal

¹¹ The term “pre-graphitisation” is used in this thesis to describe thermal treatment of Waxy Oil green coke to a temperature of 2 000 °C.

porosity of the virgin sample. At $-75\ \mu\text{m}$ the catalyst still reports to this fraction, making the effect on its density easier to determine.

5.1.7 Graphitisation

High-ash Waxy Oil green coke was obtained from the commercial delayed coker at Secunda, South Africa. The green coke was dried and separated into size fractions. The size fractions were recombined to produce a composite sample (2 200 g) for graphitisation. The weights of the size fractions in the composite sample are shown below.

- 0–1 mm (400 g or 18.2%)
- 1–2 mm (400 g or 18.2%)
- 2–4 mm (400 g or 18.2%)
- 4–8 mm (400 g or 18.2%)
- > 8 mm (600g or 27.2%)

The size fractions of green coke were analysed for VCM, ash, metals and real density according to the ASTM standards shown in Table 5-1.

The graphitisation reaction was conducted by the author at Jeenel Technology Services (Pty) Ltd, Boksburg, South Africa. The sample was placed in a graphite crucible, insulated with alumina and graphite wool. The outer lid and the support of the medium-frequency induction furnace were constructed from concrete. Further insulation was provided by zirconium sand. The furnace was equipped with two outlets. The system was continually purged with argon gas.

The medium-frequency induction furnace was heated to approximately $3\ 000\ ^\circ\text{C}$ over a period of 120 min. The furnace was held at a temperature of $3\ 000\ ^\circ\text{C}$ for 90 min. The system was cooled overnight under an argon flux.

5.1.8 Standard analyses

After cooling, the graphite was removed and sieved into size fractions and the weight percentage of each fraction was recorded. The size fractions were analysed according to the ASTM standards shown in Table 5-1.

5.2 *Experimental procedures for Chapter 7*

5.2.1 Removal of solids from Waxy Oil

A 40 ℓ sample of Waxy Oil was obtained from the Sasol Synfuels delayed coker. Filtration experiments were conducted by the author on the premises of Solid Liquid Filtration Consultants (SLFC) in Randburg, South Africa. Samples of Waxy Oil (approximately 100 ml) were heated to $90\text{--}95\ ^\circ\text{C}$ prior to filtration. The filtration apparatus is composed of a loading cell (height 6 cm; diameter 7 cm) equipped with a steam jacket on the perimeter. The lid of the cell was connected to a nitrogen pressure line. The base of the cell tapered into a funnel. Sintered metal filters (7 cm in diameter) were obtained from the Mott Corporation. The experiments used filters with apertures of 2.0, 1.0 and $0.5\ \mu\text{m}$. A diagram of the experimental set-up for the filtration apparatus is shown in Figure 5.1.

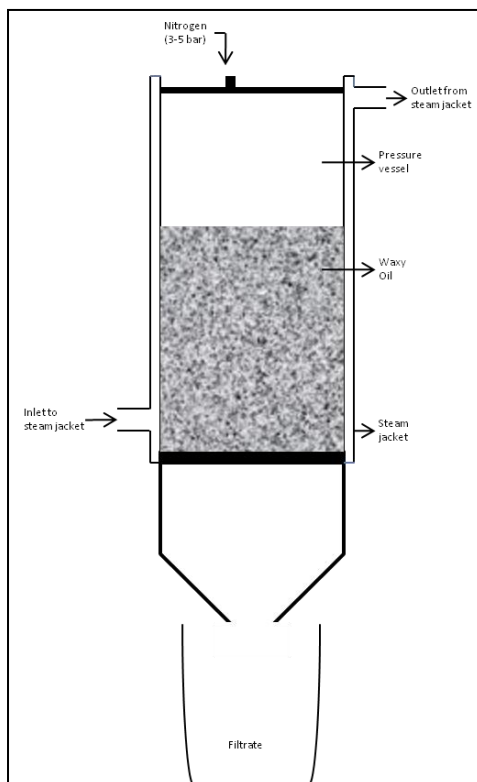


Figure 5-1 Filtration apparatus for Waxy Oil

The filter was loaded at the base of the cell and the sample (100 ml) added. The lid was fitted and a nitrogen pressure of 3–5 bar was applied. The filtrate eluted according to the micron size of the filter disc, the time being measured in minutes. The filtrate was collected in a Pyrex beaker and standard analyses were conducted at the Sasol Synfuels Process Laboratory at Secunda, South Africa. The filtration was repeated many times to obtain the amount of filtered Waxy Oil required for the modification trials. The standard test methods used to determine the characteristics of the Waxy Oil are shown in Table 5-2.

Table 5-2 Test methods used to determine the quality of Waxy Oil

Analysis	Units	Method
Matter Insoluble in Quinoline (MIQ)	Mass%	SABS 538/539
Ash content	Mass%	ASTM D-2415
Metals content	Mass%	UOP 927-92

5.2.2 Waxy Oil distillation¹²

Filtered Waxy Oil (as described in Section 5.1.1) was vacuum distilled to increase the viscosity and remove lighter hydrocarbons. Approximately 250 g of Waxy Oil was placed in a 500 ml round-bottomed flask. The distillation equipment was standard, consisting of a condenser and a receiving glass phial for distillates (submerged in ice water). The vacuum

¹² The research for Chapter 8 (Sections 8.2.2.1 to 8.5) and Chapter 9 was conducted by the author at the Instituto Nacional del Carbón (INCAR) in Oviedo, Spain, under the supervision of Dr Ricardo Santamaria.

used was -0.9 kPa. Two distillations were conducted to residue temperatures of 340 and 380 °C respectively. After distillation, the residue and distillate were weighed to determine the yields.

A photo of the vacuum distillation equipment is shown in Figure 5-2.



Figure 5-2 Photo of vacuum distillation equipment

Analysis of the distillates and residues is described in Section 5.2.4.

5.2.3 Waxy Oil thermal treatment

Waxy Oil (approximately 20 g) was placed in glass test tubes. The test tubes were placed in a reactor and the lid was closed with bolts. The reactor was connected to a distillate receiver. A photo of the thermal treatment apparatus is shown in Figure 5-3.



Figure 5-3 Photo of thermal treatment apparatus

Table 5-3 lists the experimental conditions for the thermal treatments.

Table 5-3 Experimental conditions for the thermal treatments

Experiment number	Temperature (°C)	Time ¹ (h)	Pressure (bar)
D1	400	2	5
D2	430	2	5
D3	410	2	5
D4	420	2	5
E1a	410	2	1 h at 5 bar; 1 h at 1 bar
E2	410	2	1 h at 5 bar; 1 h at 0 bar
E1b	none	none	E1a N ₂ strip to max 325 °C

¹Duration of thermal treatment at maximum heat treatment temperature

5.2.4 Analysis of modified Waxy Oils

5.2.4.1 Fourier Transform Infra-Red spectroscopy (FTIR)

FTIR was conducted on modified Waxy Oil residues using a Nicolet 8700 DTGS with a Thermo-scientific accessory. Data were collected from 4000–400 cm⁻¹. The data were used to calculate the Aromaticity Index (I_{ar}).

5.2.4.2 ^1H Nuclear Magnetic Resonance spectroscopy (NMR)

Samples were characterised by liquid-state NMR ^1H spectroscopy. CDCl_3 was used as solvent and tetramethylsilane (TMS) as the chemical shift reference. Each sample was taken into solution in a proportion of 20 wt% and placed in a 5 mm NMR tube. A 400 MHz AMX Bruker NMR spectrometer was used.

5.2.4.3 Thermogravimetric Analysis

Thermogravimetric analysis (TGA/DTG) of modified Waxy Oil residues was conducted in triplicate using a STD2960 Simultaneous DSC-TGA (the sample boat was made of steel) under the following conditions:

- 0–1 000 °C ($10\text{ °C}\cdot\text{min}^{-1}$)
- 30–50 mg sample
- 100 ml $\text{N}_2\cdot\text{min}^{-1}$

5.2.4.4 Procedure for Gas Chromatography Mass Spectrometry (GCMS)

Both Waxy Oil residues and distillates were refluxed in toluene (1:3 ratio) and sieved. The GCMS analysis of the distillates and residues was conducted on an Agilent-7890A gas chromatograph equipped with an Agilent-MS 5975 mass spectrometer. The samples of the Waxy oil were further diluted to allow for the appropriate elution of heavy alkanes which without dilution may have show overlapping peaks on the GCMS trace. Qualitative analysis of independent peaks was very useful when determining the “shift” therein according to modification procedures.

The conditions for the GCMS analysis are shown in Table 5-4.

Table 5-4 Conditions for the GCMS of Waxy Oil distillates and residues

Description	Units
Stationary phase	HP-5MS (5% phenol- methylpolysilane)
Column length	30 m
Inner diameter of column	0.25 mm
Density of the stationary phase	0.25 m
Flow of the carrier gas	1.2 ml.min ⁻¹
Injection conditions (ratio)	1:100
Injection temperature	300 °C
Temperature line of transfer	320 °C
Temperature of the oven	50 to 280 °C
Temperature programme	10 min at 50 °C; 4 °C.min ⁻¹ until 280 °C
Molecular weight range	50 to 400 uma

5.3 *Experimental procedures for Chapter 8*

5.3.1 “Static” carbonisation of modified Waxy Oils

Modified and virgin Waxy Oil samples as described in Chapter 8 (approximately 50 g) were carbonised in Pyrex glass test tubes within a stainless steel reactor (described in Section 5.1.3). A thermocouple was placed in the Waxy Oil to monitor the temperature. The pressure utilised was five bar for the complete reaction duration. The samples were carbonised utilising the following conditions:

- Heating rate: 3.0 °C.min⁻¹
- Final carbonisation temperature: 480 °C for 120 min
- De-coking¹³ temperature: 500 °C for 30 min

The green coke samples were removed in the glass test tube from the reactor after overnight cooling. The green coke and distillates in the test tube/distillate vessel were weighed to determine the respective yields. The green coke was removed from the glass tube by cracking it lightly. The “tube” of green coke was cut down the longitudinal plane for further testing

¹³ Decoking is a procedure conducted after carbonisation in which the temperature is increased by approximately 20 °C to drive off excess volatile carbon matter and make separation of the test tube and coke easier.

(especially referring to optical microscopy thereof). Green coke analyses were conducted according to procedures shown in Section 5.1.3.

5.3.2 Calcination

Green cokes A and B (approximately 10 g) were calcined in a Xerion tube furnace using the following conditions:

- Heating rate $20\text{ }^{\circ}\text{C}\cdot\text{min}^{-1}$
- Maximum temperature: $1\ 300\text{ }^{\circ}\text{C}$ for 2 h
- Argon flow: $150\text{ ml}\cdot\text{min}^{-1}$
- Overnight cooling

Calcined coke analyses were conducted according to procedures shown in Section 5.1.5.

5.3.3 Green and calcined coke characterisation

5.3.3.1 Macrostructure

Photos of the green and calcined coke macrostructure were taken along a longitudinal section of the whole green coke sample. The photos were taken using a KL 1500 LCD light source and an Olympus S2 camera.

5.3.3.2 Optical microscopy

Optical microscopy on the green and calcined cokes was conducted in the same manner. Longitudinal sections of the whole piece of coke were cut and mounted in epoxy resin using a Buehler mounting press ($150\text{ }^{\circ}\text{C}$; 29 MPa ; 15 min).

The mounted samples were polished using a series of friction media detailed below:

- Grit 120 for 1 minute
- Grit 1200 for 2 min
- Grit 2500 for 2 min
- Alumina powder solution ($-0.3\ \mu\text{m}$) for 2 min
- Alumina powder solution ($-0.05\ \mu\text{m}$) for 2 min

Optical microscopy was conducted on polished samples using a Zeiss Axioplan microscope with a Liera DC100 monitor. Micrographs were taken from the bottom to the top of the green coke particle using a computerised automatic step counter every $14\ \mu\text{m}$ along the length in polarised light and representative micrographs taken with a 10x to x50x objective lens. The percentage of mosaic and flow domains was calculated compared for each micrograph. Micrographs were taken down the length of the coke section and flow domains were the dominant microstructure towards the top of the coke section. Thus, the percentage of micrographs where flow domains were the dominant microstructure compared with mosaics (at the bottom of the coke section) could be calculated to produce a microstructural height profile of the coke section.

Polarised light microscopy was used to determine the difference in the texture of the coke samples. This was conducted using a polarizer between the light source and the mirror. A half wave retarder was additionally used placed between the analyser and the mirror. Polarised light microscopy observes the interference colours due to the variance in the orientation of the graphitic lamellae. Examples of light in the visible spectrum being established due to interference include:

- Purple when the light is reflected perpendicular to the graphite lamellae
- Yellow when the light is reflected to the right of the graphitic lamellae
- Blue when the light is reflected to the left of the graphitic lamellae

Other colours of the visible spectrum may be observed depending on the orientation of the graphitic lamellae for example red. The catalyst is seen as a white colour.

Isotropic cokes appear as small circular areas with the same red colour while anisotropic carbons for example needle coke show oriented flow domains across the micrograph. During polarized microscopy three objective lenses were utilized as described below:

- 10x objective (or 100x magnification) in air using a scale of 100 microns
- 20x objective (or 200x magnification) in air using a scale of 50 microns
- 50x objective (or 500x magnification) using oil immersion and a scale of 20 microns.

In terms of the repeatability and representative nature of the micrographs the longitudinal section of the coke was observed in the middle and to either side thereof to determine an average micro texture.

5.3.3.3 Carboxy (carbon dioxide) and oxidative consumption of carbon

A longitudinal section of calcined coke was ground and sieved to $-200\ \mu\text{m}$. The carboxy reactivity was conducted in the TGA under the following conditions:

- 40–1 000 °C
- Heating rate: $10\ \text{°C}\cdot\text{min}^{-1}$
- Nitrogen flow: $150\ \text{ml}\cdot\text{min}^{-1}$
- Carbon dioxide flow: $150\ \text{ml}\cdot\text{min}^{-1}$, or air flow: $150\ \text{ml}\cdot\text{min}^{-1}$
- Isothermal condition for 2 h at 1 000 °C

5.3.3.4 Raman spectroscopy

Raman spectra were obtained in a high-resolution Raman microscope Jobin Yvon Horiba. Extended scans from $500\text{--}3500\ \text{cm}^{-1}$ were performed to obtain the first- and second-order region of the Raman spectrum of the materials, with typical exposure times of 5 s. Measurements were made on the different parts of the samples embedded in resin, ground with different SiC grades and subsequently polished to $0.05\ \mu\text{m}$ with alumina. A microscope was used to focus the excitation laser beam (green line of an argon laser $\lambda = 532\ \text{nm}$) on the sample. The band intensity, position and width were determined using a mixed Gaussian-Lorentzian curve-fitting procedure. The degree of disorder was estimated from the relationship I_D/I_T , where I_D corresponds to the intensity of the D band ($1350\ \text{cm}^{-1}$) and I_T corresponds to the total intensity of all first-order region bands (D, G, D' at 1350 , 1580 and $1620\ \text{cm}^{-1}$ respectively).

5.3.3.5 Scanning Electron Microscopy (SEM)

SEM was performed in a Zeiss DSM 942 microscope, equipped with conventional SE (secondary electrons), solid state (two sectors) and polar BSE (backscattered electrons) signals. Chemical analyses were performed by X-ray energy dispersive analyser coupled to the SEM detector. The polished surfaces of the coke were coated with gold prior to the SEM.

5.4 *Experimental procedures for Chapter 9*

5.4.1 Filtration and thermal treatment

Virgin Waxy Oil was heated to approximately 100 °C and filtered through a 1 µm plate. The filtrate was thermally treated in a 1 ℓ reactor with connection to a distillate vessel at 410 °C, 5 bar for 2 h. The residue was vacuum distilled to remove lighter cracked molecules at 420 °C with a negative vacuum of 0.9 kPa.

5.4.2 Low-temperature carbonisation

The residue of vacuum distillation was thermally treated in test tubes (in a 1 ℓ reactor connected to a distillate vessel) using approximately 50 g of feed. The carbonisation was conducted at different times, namely 10, 20, 40, 60 and 120 min at 450 °C at a pressure of 5 bar. The test tubes were removed after cooling and weighed to determine the yield.

5.4.3 Thermogravimetric Analysis (TGA) and Differential Thermal Gravimetry (DTG)

Samples of the residue were obtained from the various test tubes and crushed. The TGA/DTG was conducted on representative samples in accordance with the procedure reported in Section 5.2.4.3.

5.4.4 Fourier Transform Infra-Red (FTIR) Spectroscopy

The Aromatic Index (I_{ar}) of the residue was determined using the procedure described in Section 5.2.4.1

5.4.5 Procedure for Gas Chromatography Mass Spectrometry (GCMS)

GCMS was conducted according to the procedure described in Section 5.2.4.4, except for the fact that NMP was used as the solvent and not toluene.

5.5 *Concluding remarks – Experimental*

The results of the experimental procedures listed above are reported and discussed in Chapters 6 to 9.

6 INFLUENCE OF CATALYST CONCENTRATION ON THE CHARACTERISTICS OF WAXY OIL COKE^{14,15}

6.1 Introduction

This chapter examines the effect of iron oxide content (as determined by the ash content) on the physical/chemical characteristics of commercial Waxy Oil green coke and thermally treated variants thereof. Green cokes were thermally treated to 1 400 °C (termed “calcined coke”) and 2 000 °C (termed “pre-graphite”¹⁶). Green coke was further thermally treated to 3 000 °C to determine the percentage reduction in the ash and iron content of Waxy Oil graphite.

The ash content of Waxy Oil calcined coke (as reported in this chapter) is at least an order of magnitude higher than that of the needle coke specification. However, as no scientific evaluation of Waxy Oil coke has previously been conducted, determination of the ash content is a prerequisite since it provides a template against which the effect of interventions (detailed in later chapters) may be compared.

Four commercial Waxy Oil green coke samples with increasing ash contents were obtained. The sample numbers and ash contents of the green coke are shown below.

- Sample 1: Ash content (1.84%)
- Sample 2: Ash content (4.22%)
- Sample 3: Ash content (7.47%)
- Sample 4: Ash content (11.19%)

6.2 Macrostructure of needle coke

The ability to show preferred orientation on a macro (visual) scale is characteristic of needle cokes as shown in Figure 6-1.

¹⁴ The research described in this chapter was presented at Carbon 2010, “From Nano to Macro” the Annual World Conference on Carbon, Clemson University, South Carolina, USA, 11–16 July 2010 (JG Clark, B Rand, MP Hayes, W Barnard, S Lubhelwana).

¹⁵ The research described in this chapter was presented at the 15th Coal Science and Technology Conference Indaba 2010, “Clean Coal, Clean Energy”, 17–18 November 2010 (JG Clark, B Rand, MP Hayes, W Barnard, S Lubhelwana).

¹⁶ The term “pre-graphite” is used to describe Waxy Oil coke thermally treated at 2 000 °C. It is distinguished from the term “calcined coke” (treated at 1 400 °C) and “graphite” (thermally treated at 3 000°C, as reported in Chapter 7).

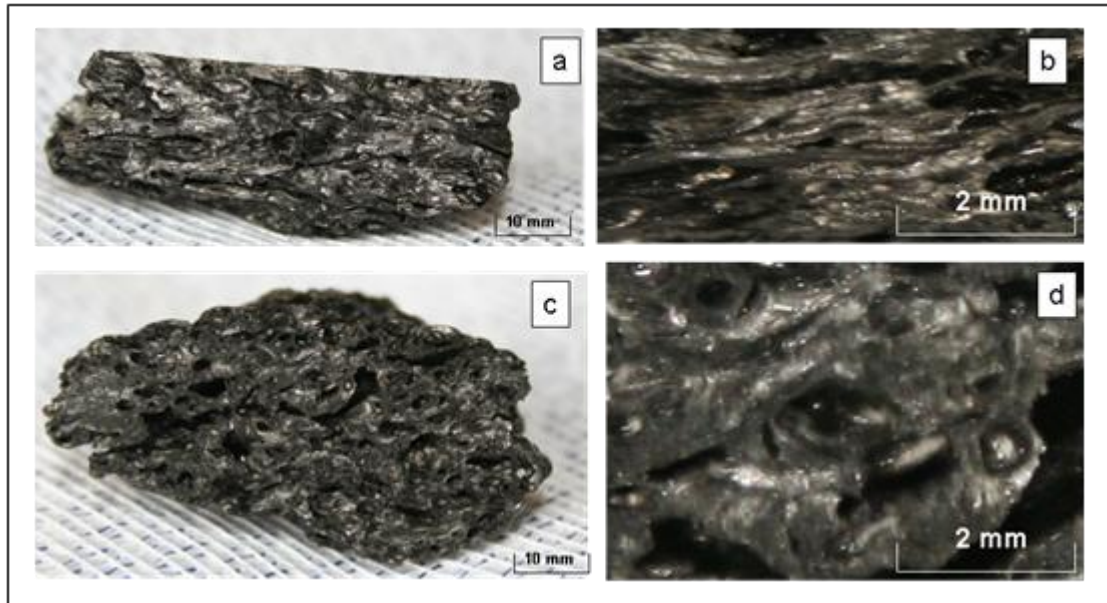


Figure 6-1 Photos of commercial needle coke in the longitudinal direction (a and b) and in the transverse direction (c and d)

Visual examination of needle coke shows flow domains and parallel pore morphology (Figure 6-1a), which become even more evident at a slightly higher magnification (Figure 6-1b). However, the converse is evident in the transverse orientation. The visual cross-section of needle coke (Figure 6-1c) does not show preferred orientation. Under slightly higher magnification (Figure 6-1d), the concentric pattern of carbon planes around a central pore is evident. The photos in Figure 6-1 serve as a template against which the macrostructure of the four Waxy Oil cokes may be compared, as discussed below.

6.3 Macrostructure of Waxy Oil green coke

A piece of high-ash green coke (approximately 70 mm in diameter) from each of Samples 1 to 4 was cut in three separate orthogonal planes in order to represent randomly ascribed X, Y and Z planes. Photos were taken of each of these planes (Figures 6-2 to 6-5).



Figure 6-2 Photos (a-c) of Waxy Oil green coke (Sample 1; 1.841% ash) on an X-, Y- and Z-axis

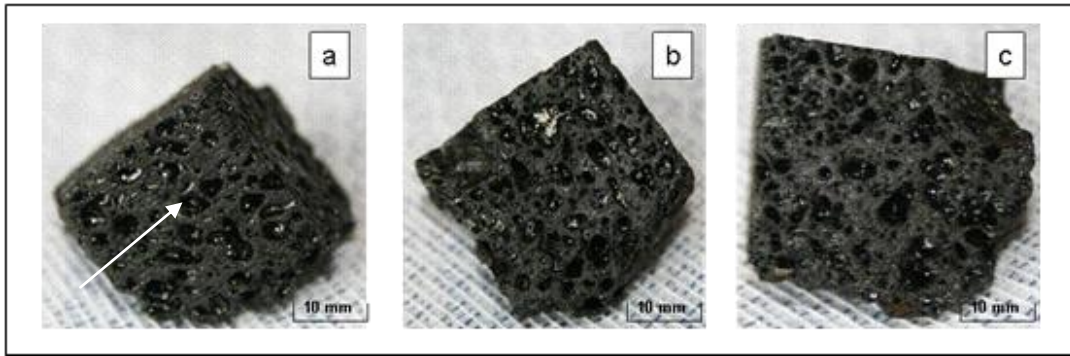


Figure 6-3 Photos (a-c) of Waxy Oil green coke (Sample 2; 4.223% ash) on an X-, Y- and Z-axis

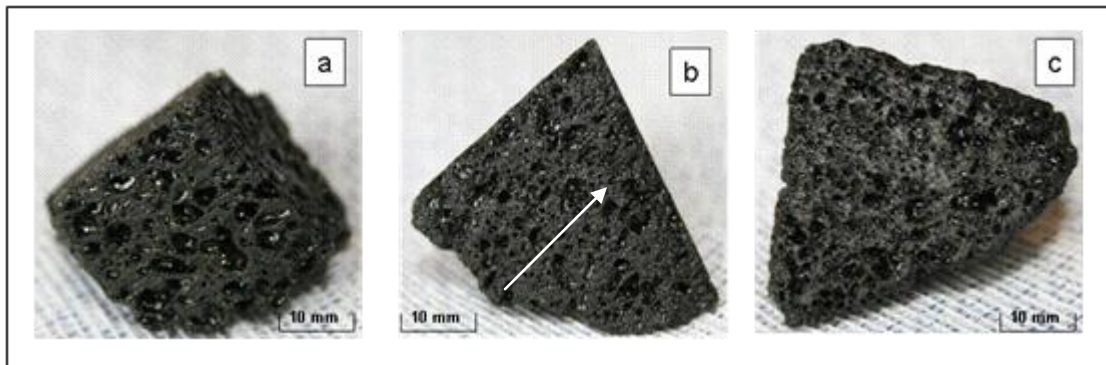


Figure 6-4 Photos (a-c) of Waxy Oil green coke (Sample 3; 7.471% ash) on an X-, Y- and Z-axis

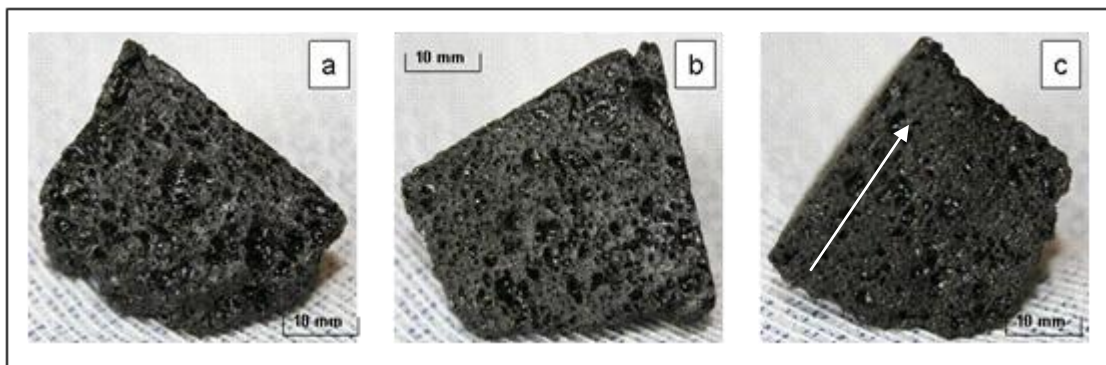


Figure 6-5 Photos (a-c) of Waxy Oil green coke (Sample 4; 11.186% ash) on an X-, Y- and Z-axis

The four high-ash Waxy Oil green cokes exhibit the macro-appearance of a sponge coke (in terms of macropore morphology), and the preferred macro-orientation of the carbon domains is not immediately distinguishable. However, there are slight indications of preferred orientation on one of the planes as indicated by the arrow in Figures 6-2a, 6-3a, 6-4b and 6-5c. There is no visual effect of the increasing ash content on the macrostructure of the four Waxy Oil cokes. The indication of preferred orientation of the Waxy Oil green coke carbon planes is, however, not supported by the parallel orientation of pores as is typical of needle coke (Figure 6-1). Waxy Oil green cokes appear highly porous (in comparison with the needle coke shown in Figure 6-1) due to the low green coke yield (18% from the fresh Waxy Oil feed to the delayed coker).

6.4 Chemical analysis of Waxy Oil green cokes

Analysis of the four Waxy Oil green coke samples is shown in Table 6-1.

Table 6-1 Analysis of Waxy Oil green cokes

	Units	Sample 1	Sample 2	Sample 3	Sample 4
Carbon	Mass%	90.200	90.800	89.200	85.600
Hydrogen	Mass%	3.680	3.680	3.520	3.630
Nitrogen	Mass%	0.050	0.030	0.083	0.020
Sulphur	Mass%	0.005	0.004	0.006	0.007
Ash content	Mass%	1.84	4.22	7.47	11.19
Volatiles (VCM)	Mass%	8.11	8.69	8.97	11.65
Fixed carbon¹	Mass%	90.05	87.09	83.56	77.17
Inherent moisture	Mass%	0.20	0.19	0.19	0.23
Real density (-75 µm; helium)	g.cm⁻³	1.3879	1.4237	1.456	1.4792

1) Fixed carbon = 100% - (ash + VCM)

The ash contents of the Waxy Oil green cokes increase from Sample 1 to Sample 4 (from 1.84 to 11.19%), with a reciprocal decrease in the fixed carbon content (from 90.05 to 77.17%) due to the increasing catalyst content. The high ash content of Samples 1 to 4 deems these green cokes commercially inappropriate for calcining (in respect of current recarburiser specifications). The VCM of Samples 1 to 3 (from 8.11 to 8.97%) is within the expected commercial range (6–9%), while that of Sample 4 (11.65%) is slightly higher. There is no correlation between the ash and the Volatile contents.

Both the nitrogen content (0.030–0.083%) and sulphur content (0.004–0.007%) of Samples 1 to 4 are comparatively lower than those of most green cokes produced either from petroleum crude oil or coal-tar origins.

The real density of the coke samples is determined by a -75 µm PSD (particle size distribution), thus negating much of the variability associated with particle size and macroporosity. As shown in Table 6-1, there appears to be a correlation between an increase in the real density (1.3879 to 1.4792 g.m⁻³) from Sample 1 to Sample 4 and in the ash content (1.84 to 11.18%) respectively. Plotting a linear regression of the relationship between the real density against the ash content indicates a good linear correlation ($R^2 = 0.9655$). This is to be expected since the inorganic impurities have a higher density than the carbon.

6.4.1 Thermogravimetric Analysis (TGA) of Waxy Oil green cokes

TGA of Samples 1 to 4 was conducted to investigate devolatilisation (in an inert nitrogen atmosphere) and immediately thereafter to determine the oxidative consumption of Waxy Oil coke.

The TGA is shown in Table 6-2 and represented in graphical format in Figure 6-6. The derivative (DTG) of the mass loss rate is shown in Figure 6-7. It should be noted that the ash content shown in Tables 6-1 and 6-2 will differ given the substantial variation of the sample

size. The ash content in Table 6-1 is more representative as it is conducted in-line with an ASTM standard as prescribed in Chapter 5.

Table 6-2 Thermo Gravimetric analysis (TGA) of Waxy Oil green cokes

	Units	TGA (dry base)		
		VCM	Fixed carbon	Ash
Sample 1	Mass%	10.6	88.1	1.3
Sample 2	Mass%	10.1	87.0	2.9
Sample 3	Mass%	9.9	84.8	5.3
Sample 4	Mass%	12.9	78.0	9.1

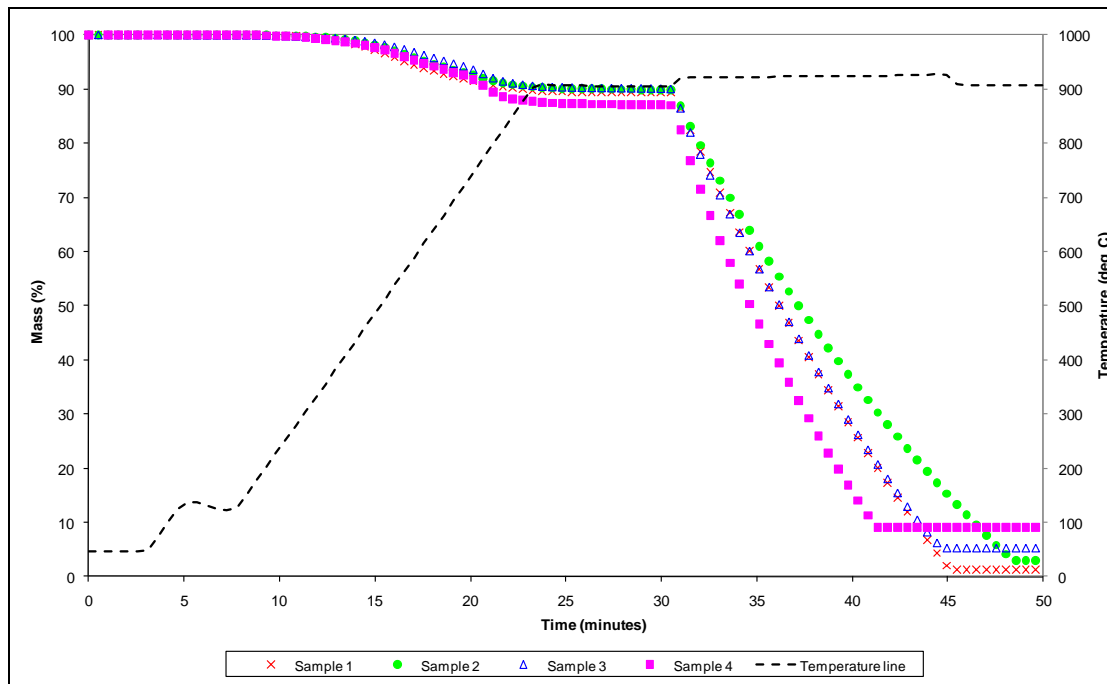


Figure 6-6 Thermogravimetric Analysis (TGA –multiple run average) of Waxy Oil green cokes

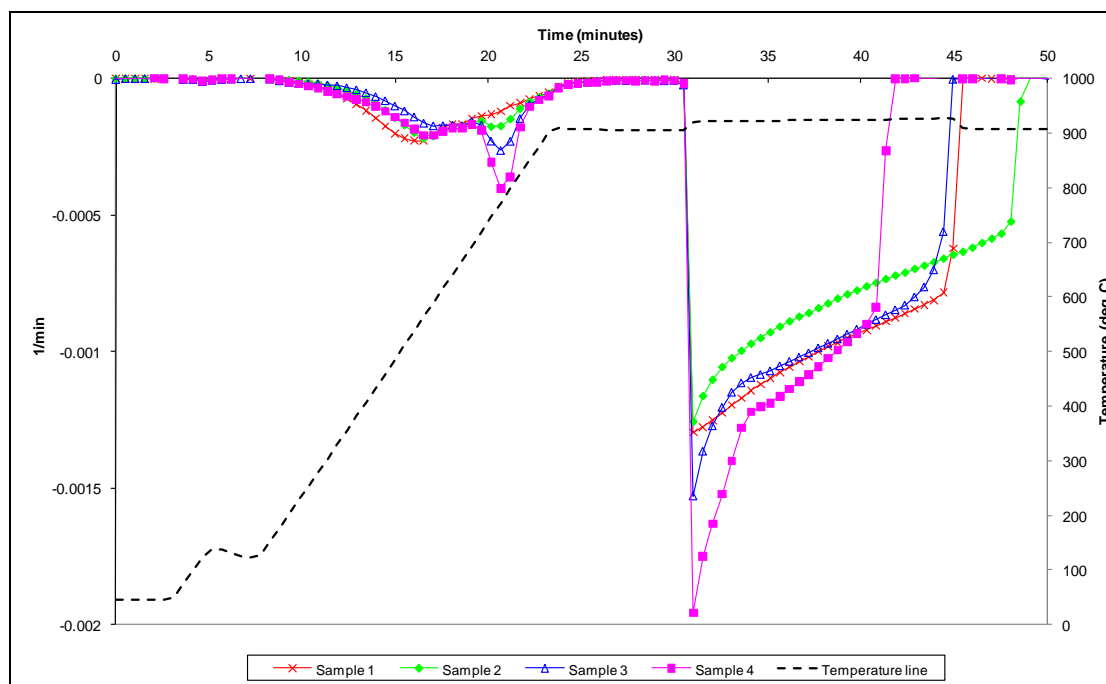


Figure 6-7 Differential Thermogravimetry (DTG multiple run average) of Waxy Oil green cokes

The proximate analysis shows an increase of the ash content with a corresponding decrease in the carbon residuum from Sample 1 to Sample 4 as indicated previously in Table 6-1. Figure 6-6 shows the mass loss of moisture and devolatilisation of VCM [starting at 8 min (≈ 150 °C) and terminating at just over 30 min (900 °C)] prior to the change in atmospheric conditions (nitrogen to air). With the change to an oxidative atmosphere, the fixed carbon is consumed until a stable residuum mass is indicated (mostly attributable to the ash content).

The DTG (Figure 6-7) shows all four cokes yielding a broad devolatilisation peak which is initiated at 150 °C and levels off at 900 °C in a nitrogen atmosphere. When the atmosphere is then changed to air, there is a steep peak of maximum reaction rate which increases in initial intensity as the catalyst concentration increases. The termination of these peaks is correlated to an increase of the catalyst content due to ash occlusion of the remaining carbon.

6.4.2 Influence of iron oxide or elemental iron on the oxidative consumption and carboxy reactivity of Waxy Oil coke

Previous research has determined that an increase in both calcium content (Boero *et al.*, 1987; Oya *et al.*, 1984; Lang & Neavel, 1982) and elemental iron (Walker *et al.*, 1983; Jenkins *et al.*, 1973) is linked to an increase in the rate of oxidative consumption and carboxy reactivity of coke.

As shown in Figure 6-7, Sample 4 (with the highest iron content) exhibited the highest initial air reactivity, followed by Sample 3 and then by Samples 1 and 2 which have lower iron and calcium contents.

The carboxy reactivity (69.78–87.02% respectively) of Waxy Oil calcined coke reported in Table 6-3 increases as the ash content (3.02–13.51%) increases from Sample 1 to Sample 4. Research conducted with petroleum sponge cokes (in the aluminium industry) confirms the catalytic effect of sodium and calcium on the carboxy reactivity of calcined coke (Hume *et*

al., 1993). The calcium content of Samples 1 to 4 increases (0.0931–0.1521%) with a corresponding increase in the carboxy reactivity. Indeed, the catalytic effect of calcium on the carboxy reactivity of petroleum cokes, coals and chars has previously been established by several authors, including Walker *et al.* (1993), Hippo and Walker (1975) and Lang and Neavel (1982). However, the increase in the calcium content may not be the only contributor to the increase in the carboxy reactivity from Sample 1 to Sample 4.

Apart from the influence of the higher comparative macroporosity, it is suggested that the unusually high iron content of the Waxy Oil calcined coke will catalyse carboxy reactivity. Iron is, by far, the element that contributes the greatest mass percentage to the ash component, on an elemental basis (Sample 1: 93.36%; Sample 2: 93.49%; Sample 3: 94.79%; Sample 4: 95.29%). It would seem unlikely that at these elevated concentrations there would be no effect (of elemental iron) on the reactivity of the coke. The author suggests three possible mechanisms by which large catalyst concentrations in the Waxy Oil coke may influence both the carboxy reactivity and the oxidative consumption.

- **As a reactivity catalyst:** Jenkins *et al.* (1973) determined that iron oxide (α -Fe₂O₃) is a poor catalyst for air and carboxy reactivity, while in its elemental form iron (Fe) is a good catalyst for both carboxy and air reactivity, in agreement with Hippo and Walker (1975) and Walker *et al.* (1983). In the Waxy Oil and during carbonisation, iron is present as Fe₃O₄, while at calcination temperatures of 1 400 °C iron oxide is partially reduced to elemental iron or Fe₃C, Fe₃O₄ and Fe₂O₃ as shown in Figure 6-15 and previously reported by Wang *et al.* (2001). Thus with increasing percentages of elemental iron in the calcined coke from Sample 1 to Sample 4, catalytic carboxy reactivity should increase as confirmed by the results shown in Table 6-3.
- **As a physical barrier:** Wang *et al.* (2001) have shown the effect of iron oxide particles presenting physical occlusions to the carbon microstructure during carbonisation. This serves to inhibit coke swelling, allowing the escape of gases and thus increasing the surface area. This characteristic has been demonstrated in the evaluation of the effect of the catalyst on the microstructure of calcined coke in the current study. Carbonisation of pitch in the presence of θ -Fe₂O₃ is known to increase the yield and decrease the anisotropy of coke due to oxidative dehydrogenation reactions (Wang *et al.*, 2001).
- **As an “oxygen reservoir”:** The partial reduction of Fe₃O₄ to θ -Fe₃C and α -Fe during calcination would release oxygen, which may increase the consumption of carbon released as carbon monoxide. The potential of Fe₃O₄ to act as an “oxygen reservoir” within green coke cannot be corroborated in any of the literature cited and thus may be of a speculative nature. However, the author suggests that the unusually high catalyst concentration of the Waxy Oil and the fact that the dominant contaminant is Fe₃O₄ would indicate that within the green coke, there is a substantial oxygen concentration.

6.5 Waxy Oil calcined coke

In order to investigate exclusively the effect of metal contaminants on the characteristics of the calcined coke, the Waxy Oil green coke samples were calcined in a muffle oven (with a nitrogen flux) at an extremely low temperature ramp rate (from ambient to 1 300 °C) as given in Chapter 5.3.2.

6.5.1 Influence of increasing catalyst content on the microstructure of Waxy Oil calcined coke

6.5.1.1 Comparative summary of the effect of the catalyst content (catalyst agglomerates¹⁷) on the microstructure of Waxy Oil calcined coke

A series of comparative micrographs of Waxy Oil calcined coke are shown in Figure 6-8 to Figure 6-11, corresponding to Samples 1 to 4 respectively. While each of the cokes presented a fair degree of heterogeneity (examined in more detail in Figure 6-14 to Figure 6-17), the micrographs shown in Figure 6-8 to Figure 6-11 are representative of the average microstructure of each of the four coke samples.

A micrograph of Sample 1 Waxy Oil calcined coke with an ash content of 3.02% is shown in Figure 6-8.

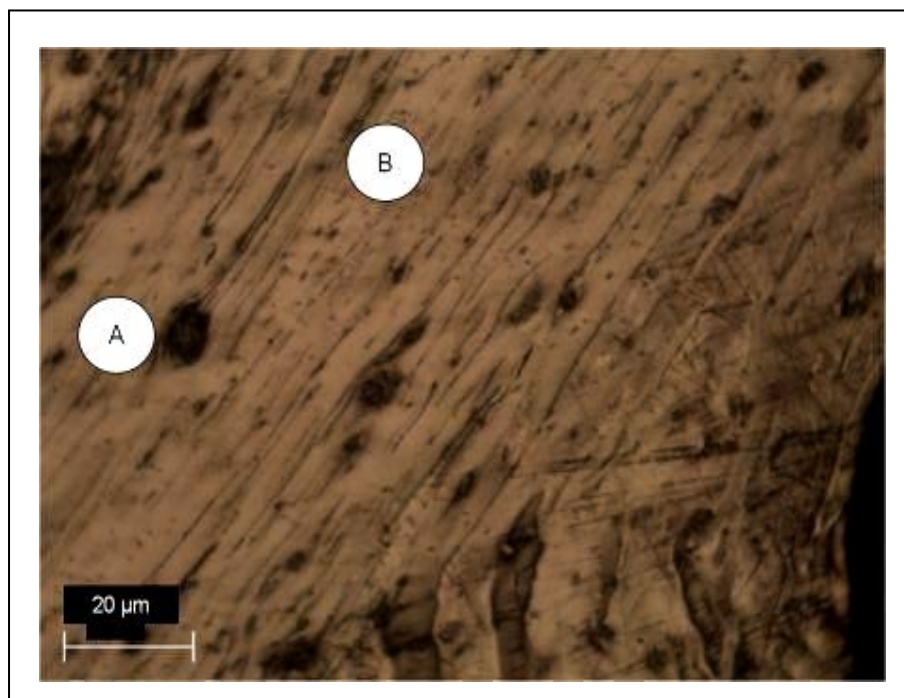


Figure 6-8 Optical micrograph of Sample 1 Waxy Oil calcined coke

The microstructure of Sample 1 is dominated by microstructural flow domains of indeterminable length as shown in Position B. The iron catalyst (appearing as black areas except for the pore on the bottom right of the micrograph) is embedded within the carbon microstructure with sizes up to 6 μm shown in Position A. The iron catalyst particles act as an obstacle to the microstructure, around which flow domains are formed.

¹⁷ The generic term “catalyst agglomerate/s” is used to describe the presence of catalyst particles within the carbon microstructure. Given the particle size distribution of the catalyst, the agglomerate should be read as consisting of either a singular catalyst particle or a grouping of catalyst particles in the same localised vicinity. It is not possible to distinguish the difference using optical microscopy.

A micrograph of Sample 2 calcined Waxy Oil calcined coke with an ash content of 5.42% is shown in Figure 6-9.

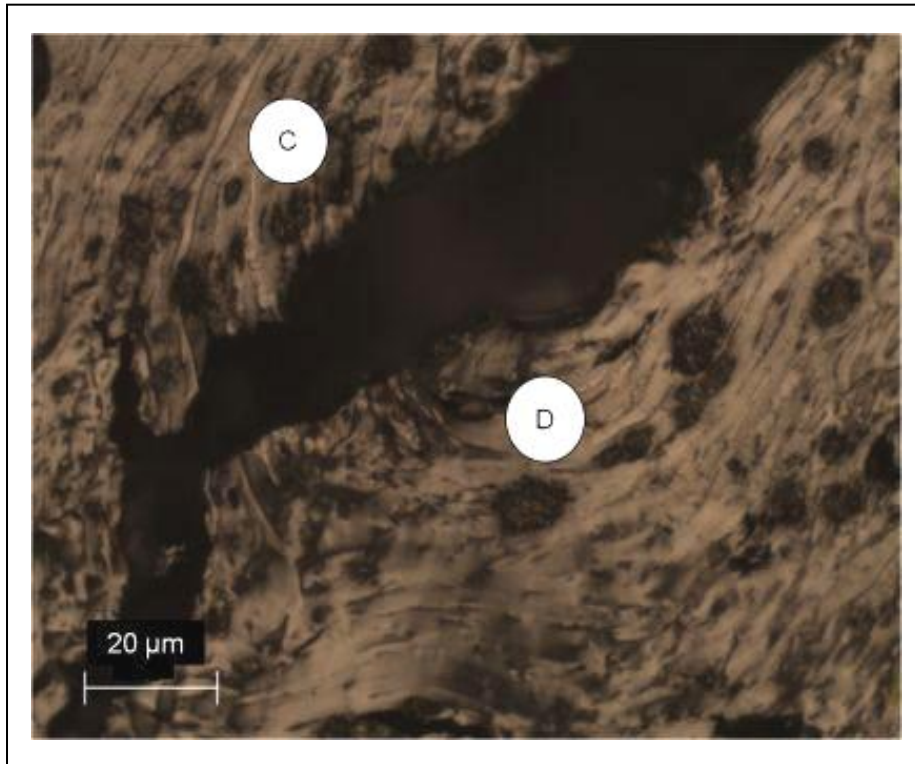


Figure 6-9 Optical micrograph of Sample 2 Waxy Oil calcined coke

As the catalyst content increases, so does the particle size (up to approximately 15 μm) and frequency as seen in the micrograph. The increase in the catalyst size may be due either to catalyst agglomeration or solely to the size of the catalyst particles. As seen in the micrograph, there is a transverse shrinkage crack separating the domain flow (Positions C and D).

A micrograph of Sample 3 calcined Waxy Oil calcined coke with an ash content of 8.66% is shown in Figure 6-10.

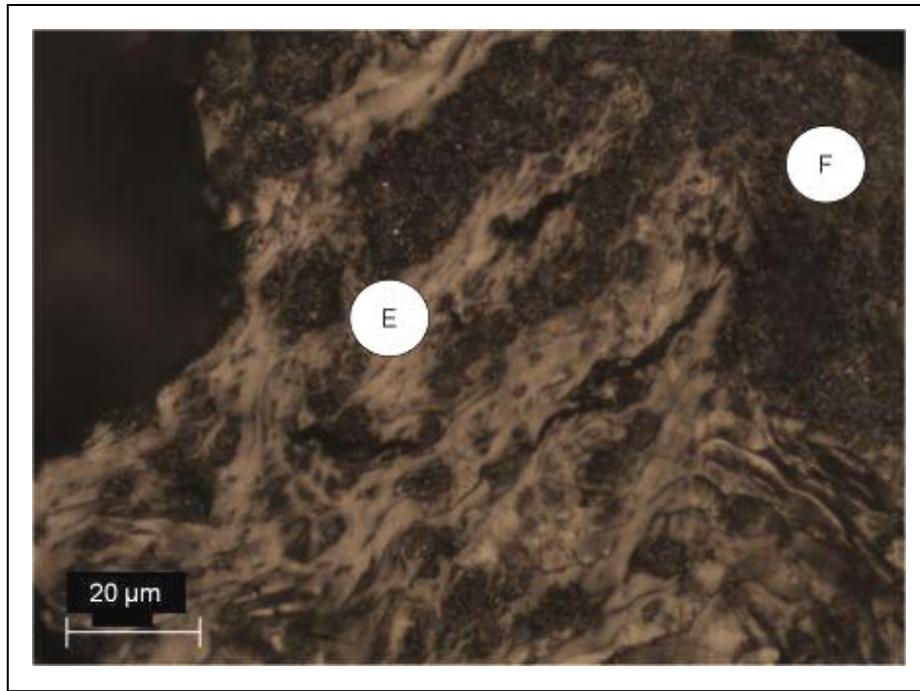


Figure 6-10 Optical micrograph of Sample 3 Waxy Oil calcined coke

Further increasing the catalyst content results in catalyst agglomerations of over 60 µm (Position F). The microstructure now represents elongated domains as shown by Position E, with smaller areas showing mosaic microstructures.

A micrograph of Sample 4 calcined Waxy Oil calcined coke with an ash content of 13.51% is shown in Figure 6-11.

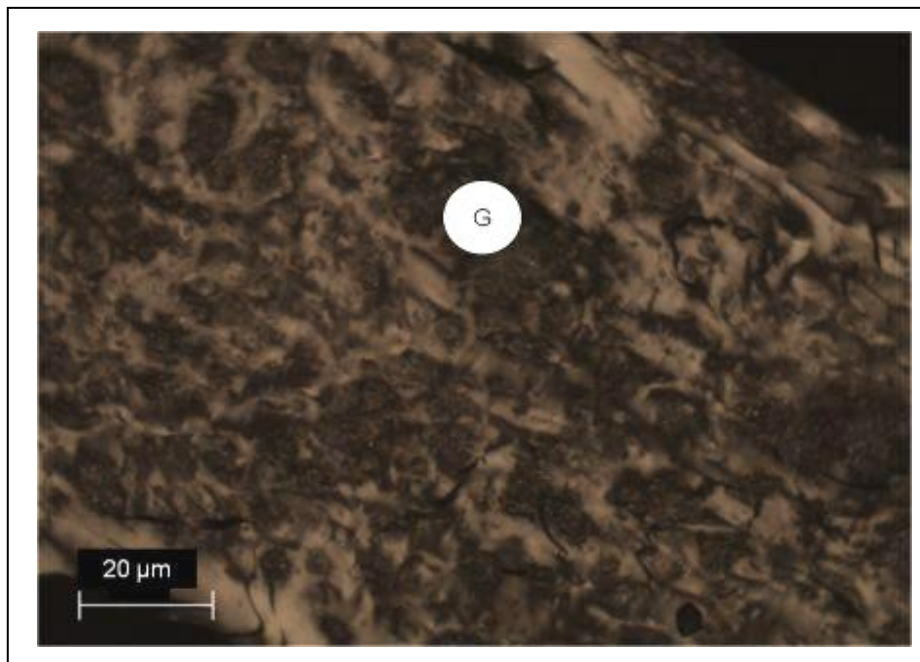


Figure 6-11 Optical micrograph of Sample 4 Waxy Oil calcined coke

In Sample 4, which has the highest catalyst content, the carbon micrograph is almost totally occluded by the matrix of catalyst agglomerates (Position G). The microstructure is heterogeneous with areas of elongated flow, coarse flow and coarse mosaic structures.

A bit map trace of catalyst agglomerates within the carbon microstructure Samples 1 to 4 of Waxy Oil calcined coke is shown in Figure 6-12.

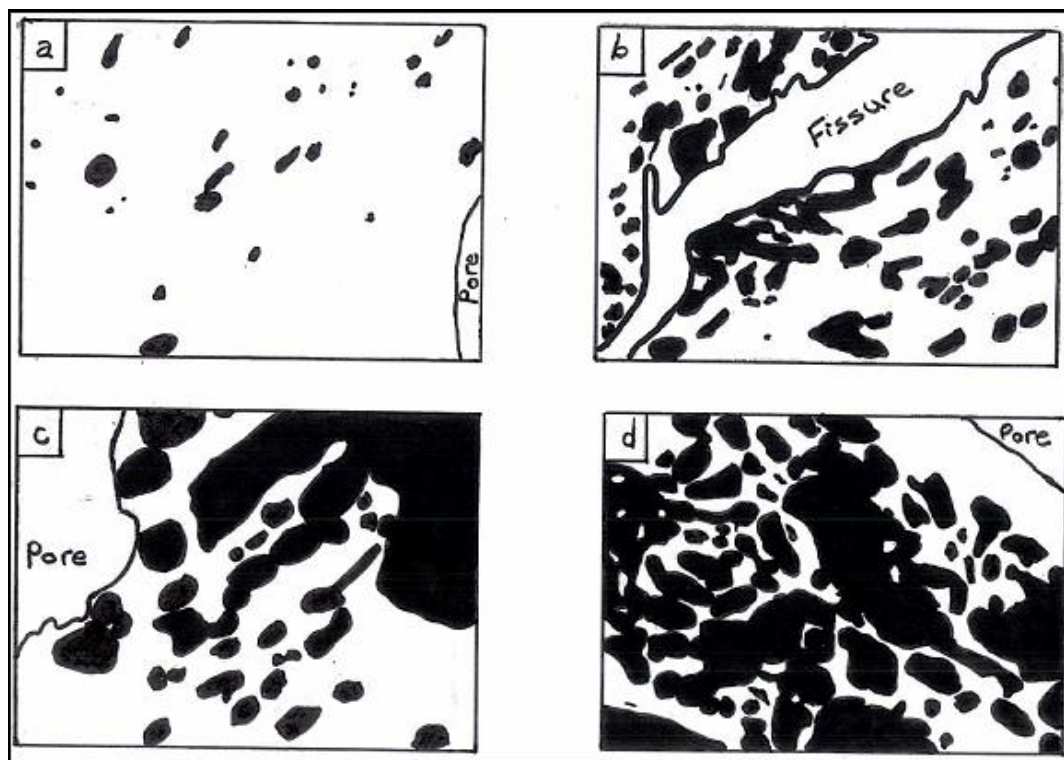


Figure 6-12 Diagram showing contamination of calcined coke by catalyst agglomerates of Samples (a) 1, (b) 2, (c) 3 and (d) 4

The catalyst content is shaded in black and shows clearly the influence of the catalyst on the spatial distribution of the carbon macrostructure. This is important when evaluating the effect of thermal graphitisation on the crystal development, discussed later in the chapter (Section 6.5.3.1).

Apart from the long-range effects of the catalyst concentration on the carbon microstructure, the internal structure of these catalyst agglomerates warrants further investigation. The internal structure of the catalyst agglomerates showing the formation of carbon mosaic microstructures is shown in Figure 6-13.

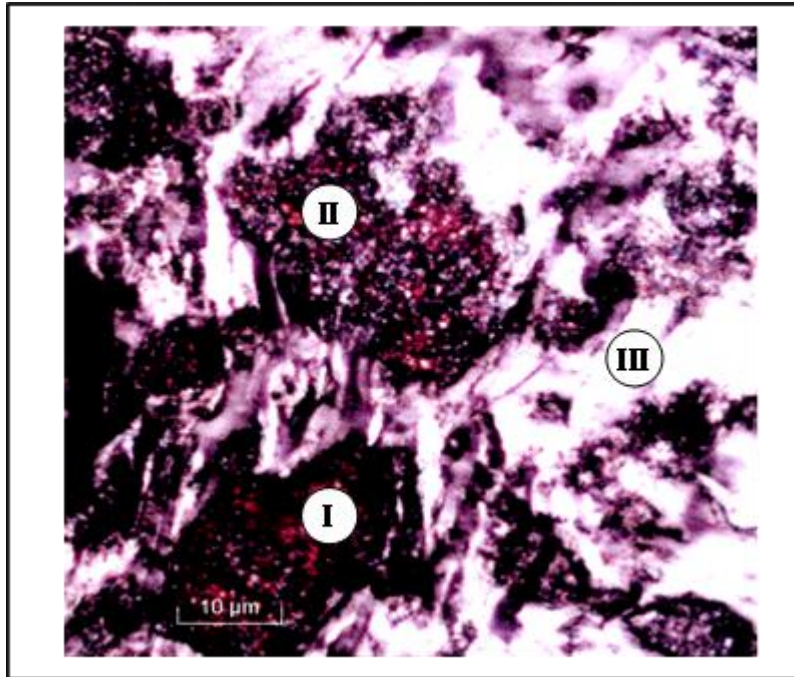


Figure 6-13 Polarised micrograph of catalyst agglomerates within the carbon microstructure

The form of the catalyst in the green coke is Fe_3O_4 . Inert calcination (1 400 °C) liberates much of the volatile carbon matter (probably by devolatilisation) and partially reduces the catalyst to a mixture of Fe_3O_4 , Fe_2O_3 , Fe or Fe_3C . The “grainy” texture of the calcined coke would provide evidence for the loss of carbon. However, the visible dominance of catalyst agglomerates in the calcined coke is expected, given that calcination was conducted under inert and not oxidative conditions. The partial reduction of Fe_3O_4 to Fe may serve as a source of oxygen for carbon burn-off. As shown in Figure 6-13, within the catalyst agglomerate there is evidence of iron oxide (Position I) appearing as a brownish-red shade with mosaic microstructures (Position II) formed by catalysed oxidative polymerisation, in agreement with the findings of Wang *et al.* (2001), as opposed to the laminar flow domains (Position III) outside the immediate vicinity of the catalyst agglomerate.

An SEM image taken at 8 KV and a magnification of 15 000 times is shown in Figure 6.14.

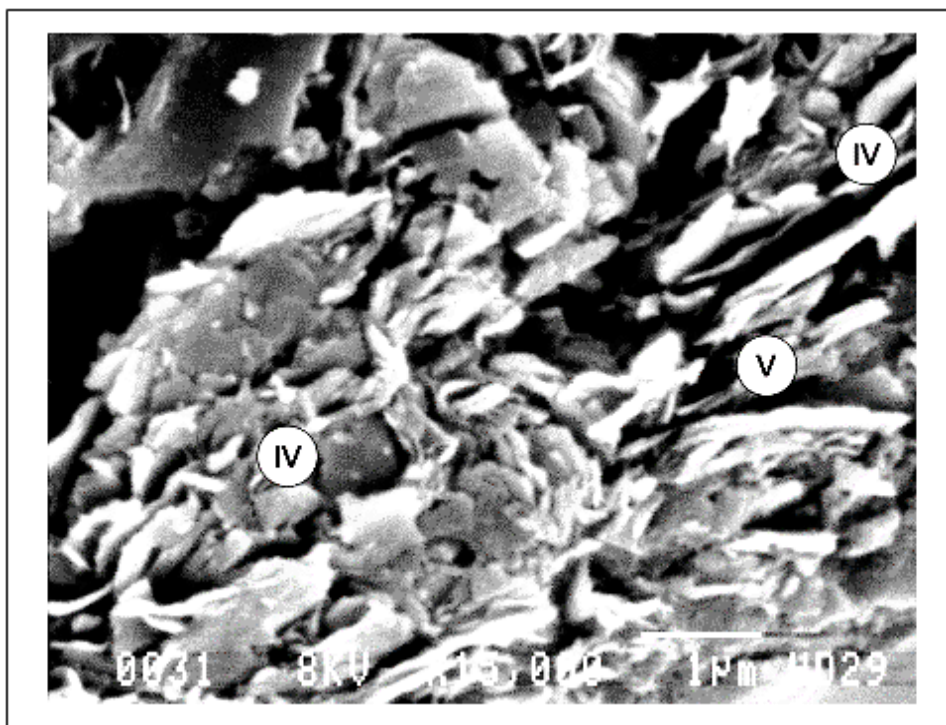


Figure 6-14 Scanning electron micrograph of ash agglomerate within the carbon microstructure of Sample 3, Waxy Oil calcined coke

The smaller catalyst particles would not be visible using optical microscopy. As shown in Figure 6-14, smaller catalyst particles less than 1 μm in diameter (Position IV – identified by their spherical nature compared to the flake like nature of the carbon microstructure) can be seen using SEM, embedded in the flake-like flow patterns of the carbon microstructure (Position V).

The author suggests that given the unusually high concentration, the catalyst (Fe_3O_4) in the green coke may serve as an “oxygen reservoir”. It is further suggested that on reduction of the metal oxide, elemental oxygen will react with any carbon molecules either within the catalyst or around the immediate perimeter and be liberated as carbon monoxide. This localised carbon burn-off in addition to the reported effect of iron (Fe) as an oxidation catalyst is in agreement with the work of Jenkins *et al.* (1973), Hippo and Walker (1975) and Walker *et al.* (1983) and is suggested as the probable cause of the high concentration. Thus the fine mosaics visible within the inner structure of the catalyst agglomerate may be partially a result of oxidative polymerisation, but may also be the carbon remnants of oxidation during calcination.

6.5.1.2 Identification of phases of the iron-based catalyst in Waxy Oil calcined coke and pre-graphite

The XRD trace of the four Waxy Oil calcined coke samples showing phases of iron is shown in Figure 6-15.

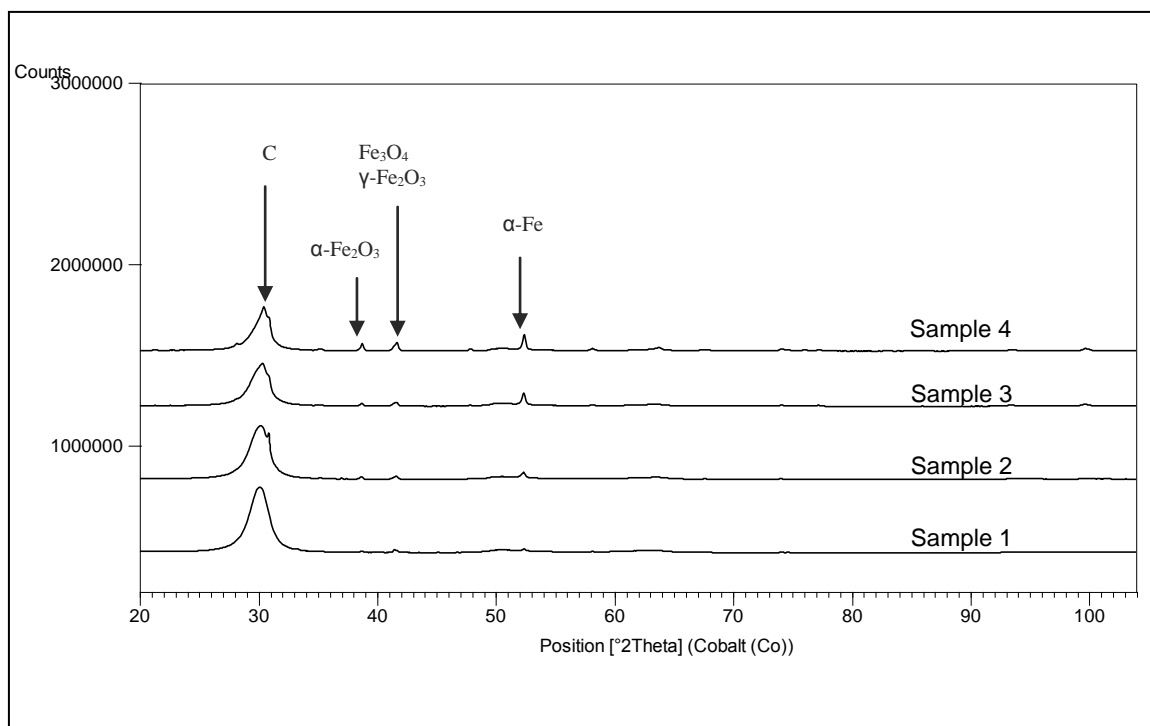


Figure 6-15 XRD trace of Waxy Oil calcined coke showing forms of the iron catalyst

Calcination induces a modification of the catalyst (Fe_3O_4) in the green coke to a mixture of Fe_3O_4 , Fe_2O_3 and Fe. However, it can be seen that as the catalyst content of the calcined coke increases (from Sample 1 to Sample 4), the peaks on the trace (allocated to the various phases of the iron-based catalyst) are more intense.

The variability of iron oxide reduction with thermal treatment has been previously reported by several authors as follows:

1. Wang *et al.* (2001) showed thermal treatment at 1 000 °C to reduce iron oxide completely to elemental iron and iron carbide. However, the surface area of the iron oxide powder (0.1–1.0 μm) may be the reason for the complete reduction at a comparatively low temperature.
2. Dhakate *et al.* (1997) showed thermal treatment at 1 400 °C to reduce iron oxide completely to elemental iron.
3. Ugarkovic and Legin (1986) showed thermal treatment at 1 500 °C to present a mixture of iron phases, including Fe_3O_4 , Fe_2O_3 and Fe.

The XRD trace of the four Waxy Oil pre-graphites showing the phases of iron is shown in Figure 6-16.

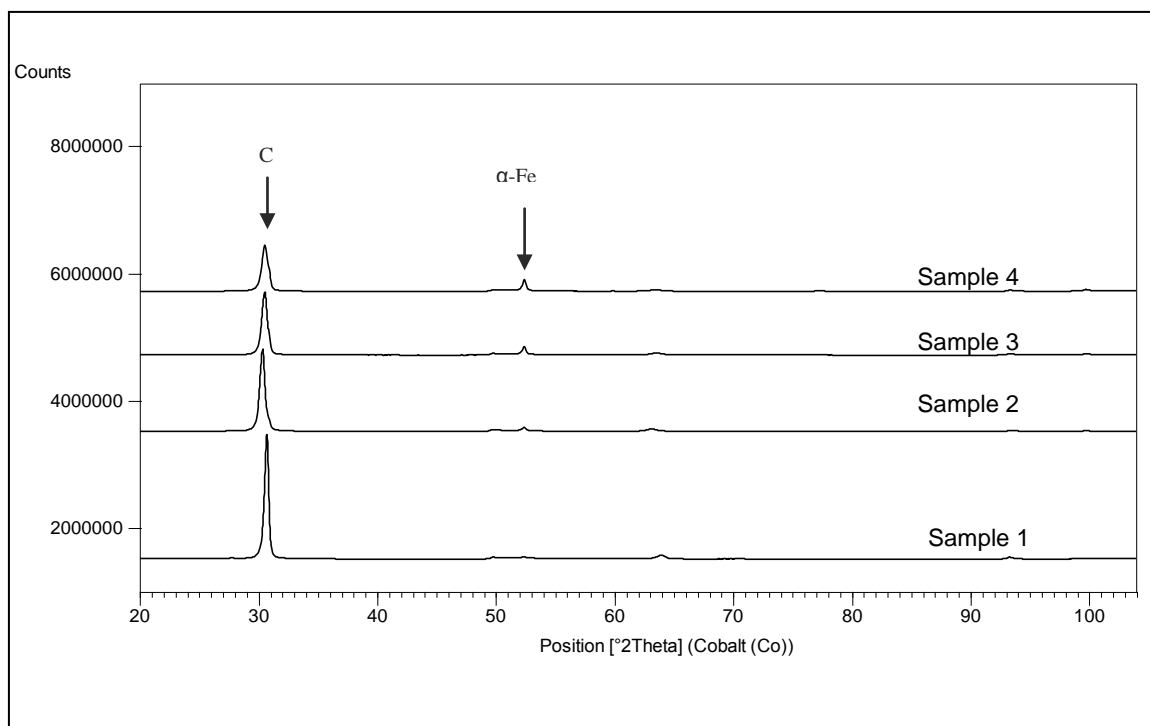


Figure 6-16 XRD trace of Waxy Oil pre-graphites showing phases of iron

Thermal treatment (2 000 °C) induced a complete reduction of the catalyst (Fe_3O_4), only yielding a peak for elemental iron. As the catalyst content of the pre-graphite increases (from Sample 1 to Sample 4), the Fe peak becomes sharper, which is expected.

It is further evident from the XRD trace that the peak in the graphite region is broader in the pre-graphite with the highest catalyst concentration and that as the concentration reduces, so the peak becomes narrower and more intense. As the catalyst concentration decreases, the spatial area for the development of microstructural anisotropy increases. This would thus indicate that the dominant graphitisation mechanism (during thermal treatment to 2 000 °C) may be thermal (depending on the microstructure) rather than catalytic, as is the case with thermal treatment at a lower temperature (1 300 °C).

6.5.1.3 Detailed examination of the heterogeneous variation in the microstructure of Waxy Oil calcined coke

While the micrographs shown in Figure 6-8 to Figure 6-11 show a representative microstructure for the four cokes, evidence of substantial microstructural variation within each of the coke samples serves to confirm the heterogeneous nature of the calcined coke samples. For this reason a more detailed analysis of the carbon microstructures is shown in Figures 6-17 to 6-20. The variation in the microstructure of Sample 1 is shown in Figure 6-17 (a–c).

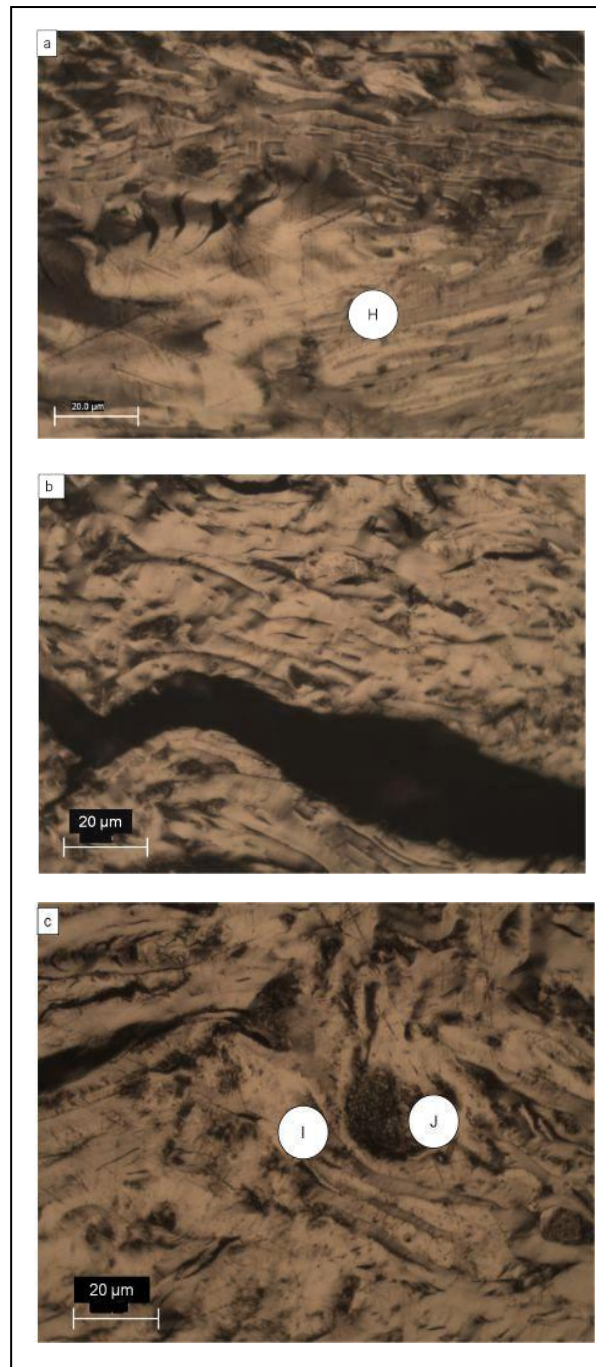


Figure 6-17 Optical micrographs (a–c) of Sample 1 of Waxy Oil calcined coke

The anisotropy of Sample 1 is dictated by the pore morphology which is parallel to the flow domains, either curved or straight (Figure 6-17a and 6-17b) respectively. However, in contrast to the “ribbon-like” morphology of needle coke, the flow domains appear shorter while the width is greater. During calcination, densification of the carbon microstructure creates ridges and valleys parallel to the flow domain (Position H). The presence of catalyst agglomerates (Position J) partially determines the morphology of the longer-range flow domains (Position I). The other contributor to the morphology of the microstructure would be the release of gases during carbonisation. Although the microstructure is dominated by acicular and elongated flow domains, there is evidence of both elongated medium and coarse

flow anisotropy. The variation in the microstructure of Sample 2 is shown in Figure 6-18 (a-c).

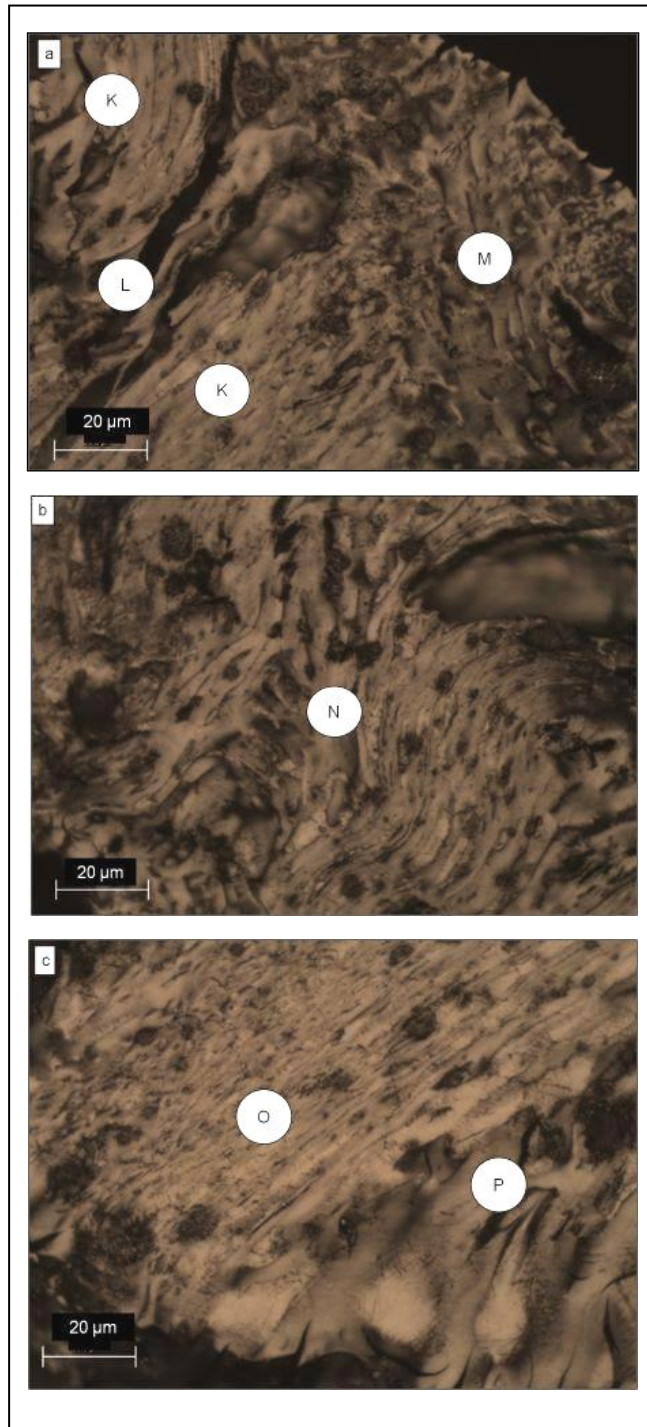


Figure 6-18 Optical micrographs (a-c) of Sample 2 of Waxy Oil calcined coke

The microstructure of Sample 2 ranges from elongated flow domains (Position K) to domains (Position M). Position N shows a central elongated domain with curved parallel domains converging from both the left and right of the micrograph. Position L shows a fissure aligned with the flow domain. Position N shows a convergence of flow domains from the left and right sides of the micrograph, with a habitual frequency of smaller catalyst particles. The

difference in the types of flow domain is seen by contrasting the longer thinner domains (Position O) and the larger wider domains (Position P).

The variation in the microstructure of Sample 3 is shown in Figure 6-19 (a–c).

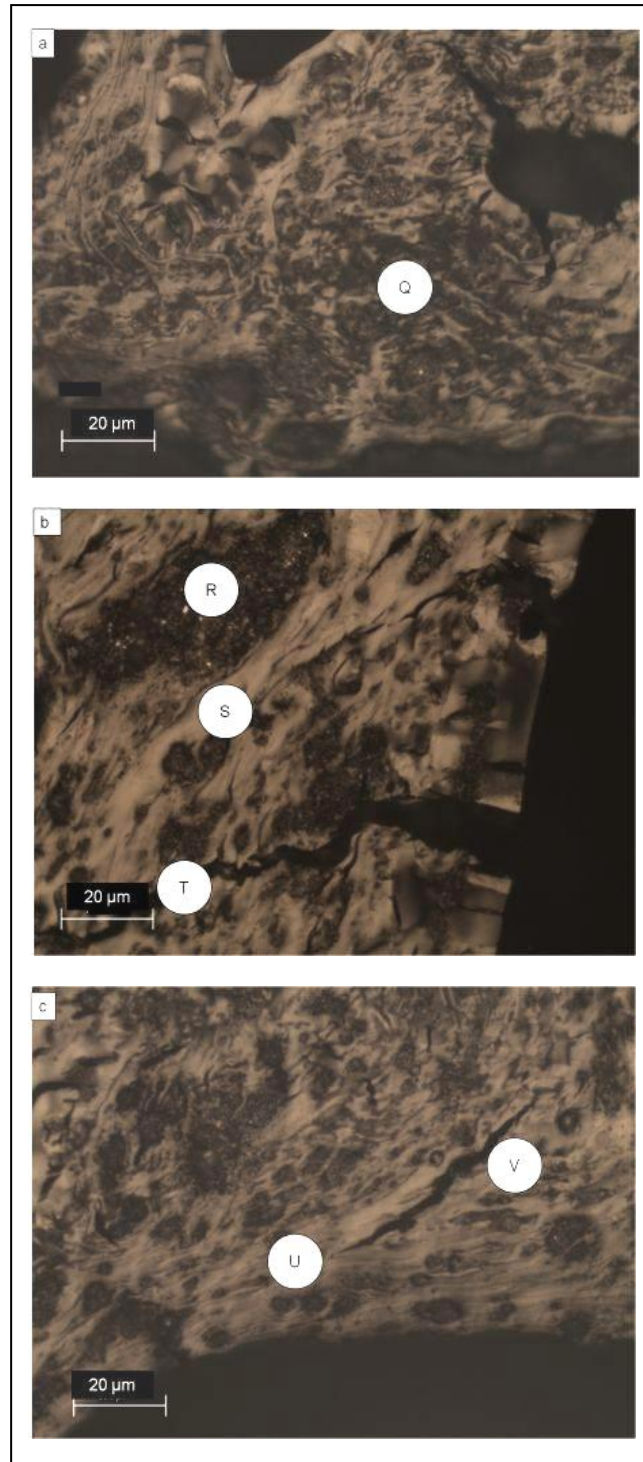


Figure 6-19 Optical micrographs (a–c) of Sample 3 Waxy Oil calcined coke

Sample 3 shows the appearance of larger catalyst agglomerates, both densely packed (Positions Q and R) and interspersed by coarse grain mosaics. As the density and size of the

catalyst agglomerates increase, the overall anisotropy of the microstructure reduces (in some areas into the mosaic range). However, in areas of the micrograph where the size and density of the ash agglomerates is low (Position S), the dominant microstructure is still elongated flow domains. The appearance of shrinkage fissures both parallel to the flow domain (Position T) and perpendicular to the flow domain (Position V and U) are similar to those described for Sample 2.

The variation in the microstructure of Sample 4 is shown in Figure 6-20 (a–c).

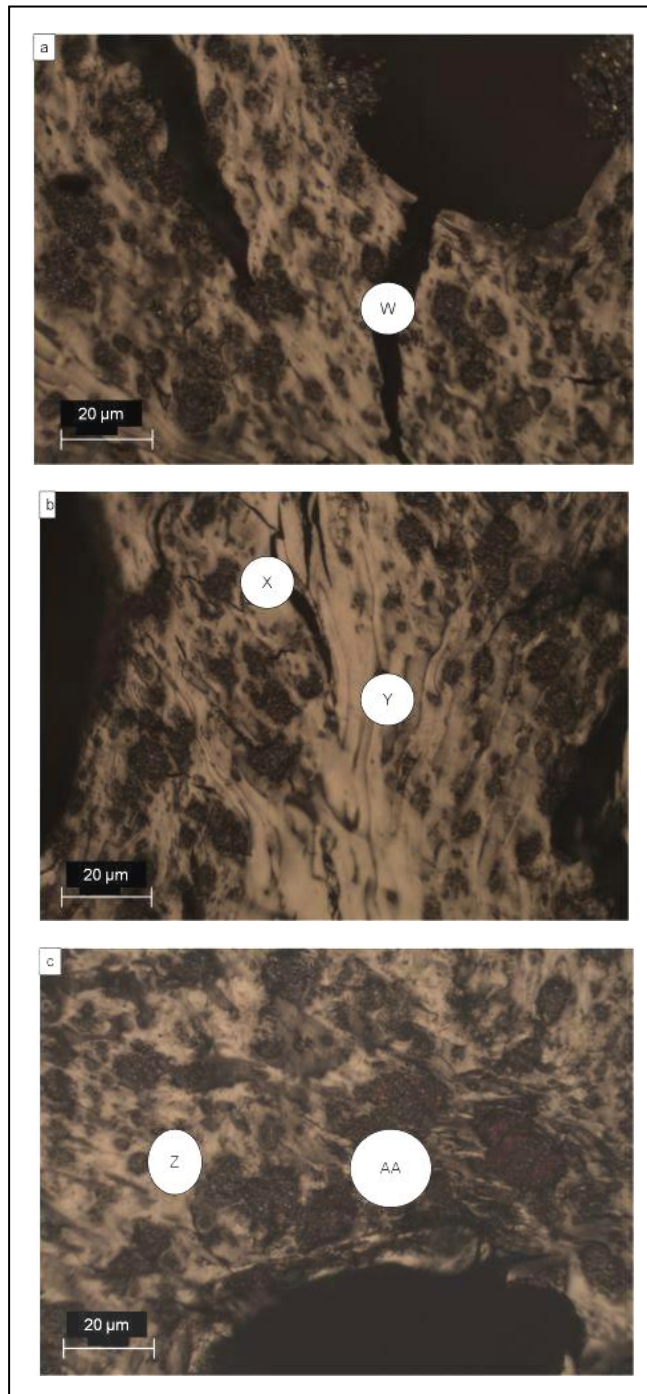


Figure 6-20 Optical micrographs (a–c) of Sample 4 of Waxy Oil calcined coke

The microstructure of Sample 4 calcined coke is highly variable, again determined by the size and density of the catalyst agglomerates, ranging from elongated flow (Position Y) to medium-grain mosaic (Position AA). Both transverse (Position W) and parallel (Position X) shrinkage fissures to the alignment of the carbon microstructure are observed. Position Z shows the close packing arrangement of the catalyst agglomerates of over 10 μm in diameter.

Thus apart from mosaic microstructures in the immediate vicinity of the catalyst agglomerate, the general microstructure appears locally anisotropic. It may therefore be argued that removing the catalyst alone would yield the anisotropic microstructure desired. However, as shown in Chapters 7 and 8, organic molecular thermal instability has a substantial effect on the microstructure. It is not seen in the above micrographs as delayed coking effectively distributes the mosaic microstructures.

6.5.2 Chemical analysis of Waxy Oil calcined cokes

The analysis of the calcined coke (Samples 1 to 4) is shown in Table 6-3.

Table 6-3 Analysis of Waxy Oil calcined cokes

	Units	Sample 1	Sample 2	Sample 3	Sample 4
Calcined coke yield	Mass%	90.6	90.5	89.4	86.5
Carbon	Mass%	97.109	95.863	94.343	92.882
Hydrogen	Mass%	0.130	0.110	0.130	0.120
Nitrogen	Mass%	0.020	0.020	0.020	0.020
Sulphur	Mass%	0.017	0.024	0.032	0.056
Real density (-75 μm ; He)	$\text{g}\cdot\text{cm}^{-3}$	2.1024	2.1087	2.1124	2.1220
Volatile Carbon Matter (VCM)	Mass%	0.57	0.47	0.38	0.59
Fixed carbon ¹	Mass%	96.41	94.11	90.96	85.90
CO ₂ reactivity	Mass%, 100 min ⁻¹	69.78	77.88	81.13	87.02
Ash content	Mass%	3.02	5.42	8.66	13.51
Metal content:					
Calcium (Ca)	Mass%	0.0931	0.1380	0.1473	0.1521
Iron (Fe)	Mass%	1.8365	2.6882	3.7474	4.7624
Silicon	Mass%	0.0308	0.0437	0.0535	0.0800
Vanadium (V)	Mass%	0.0001	0.0001	0.0001	0.0001
Nickel (Ni)	Mass%	0.0005	0.0001	0.0001	0.0001
TOTAL METALS IN COKE	Mass%	1.9671	2.8755	3.9533	4.998

Although the VCM of the four samples is relatively consistent, it does indicate slight under calcining. As expected, the ash content increases from Sample 1 to Sample 4, in agreement with the trend of the ash contents of the green coke.

The hydrogen content (0.110–0.130%) of the calcined coke shows a substantial decrease from that of the green coke (3.52–3.68%) due primarily to destructive cracking of hydrogen from the defective edges of carbonaceous layers. The nitrogen content of the calcined coke shows a slight decrease and the sulphur content a slight increase from those of the green coke form.

The real density increases from Sample 1 to Sample 4. This appears to be in contrast to the accepted relationship between a higher degree of anisotropy and higher real densities, as described by Frohs *et al.* (2007). The opposite trend is indicated in this study and is considered to be a “pseudo effect” due to the unusually high catalyst content and the smaller PSD (-75 μm) used for the analysis. As the major elemental contaminant is iron (which has a substantially higher molecular weight than carbon: 55.847 vs. 12.011 amu respectively), this is the probable cause of this unusual trend. It is also probable that given the catalyst concentration, not all the Fe_3O_4 would have been converted to either Fe_3C and Fe , which would further add to the comparative influence on the real density (as shown in the XRD of the calcined coke – Figure 6-15).

The correlation of the ash content with the real density yields a linear regression with an R^2 value of 0.9862. By using the equation to determine the regression, it is possible to predict a value for the real density ($2.0974 \text{ g}\cdot\text{cm}^{-3}$), assuming that the ash content of the coke was zero. Using the ash analysis to represent the form of the catalyst in the green coke (Fe_3O_4) may be questionable as during the ashing of the coke, Fe_3O_4 would be oxidised to Fe_2O_3 . However, it is the closest comparison. The correlation of the iron content with the real density yields a linear regression with an R^2 value of 0.9684. By using the equation to determine the regression, it is possible to predict a value for the real density ($2.0901 \text{ g}\cdot\text{cm}^{-3}$), assuming the iron content of the coke was zero. The minimal difference between both the R^2 values for the linear regressions may indicate that there is a mixture of iron compounds present (i.e. Fe_3O_4 , Fe_2O_3 , Fe_3C and Fe), as confirmed by the XRD analysis shown in Figure 6-19.

6.5.3 X-ray diffraction of Waxy Oil calcined coke

X-ray diffraction was conducted on samples of Waxy Oil calcined coke to determine the influence of the catalyst on the ordering of the crystal structure. A detailed description of the experimental protocol is given in Chapter 5, Section 5.1.5.3.

6.5.3.1 Analysis of peaks in the graphite region of Waxy Oil calcined cokes

An XRD trace of the graphite region of Waxy Oil calcined cokes is shown in Figure 6-21.

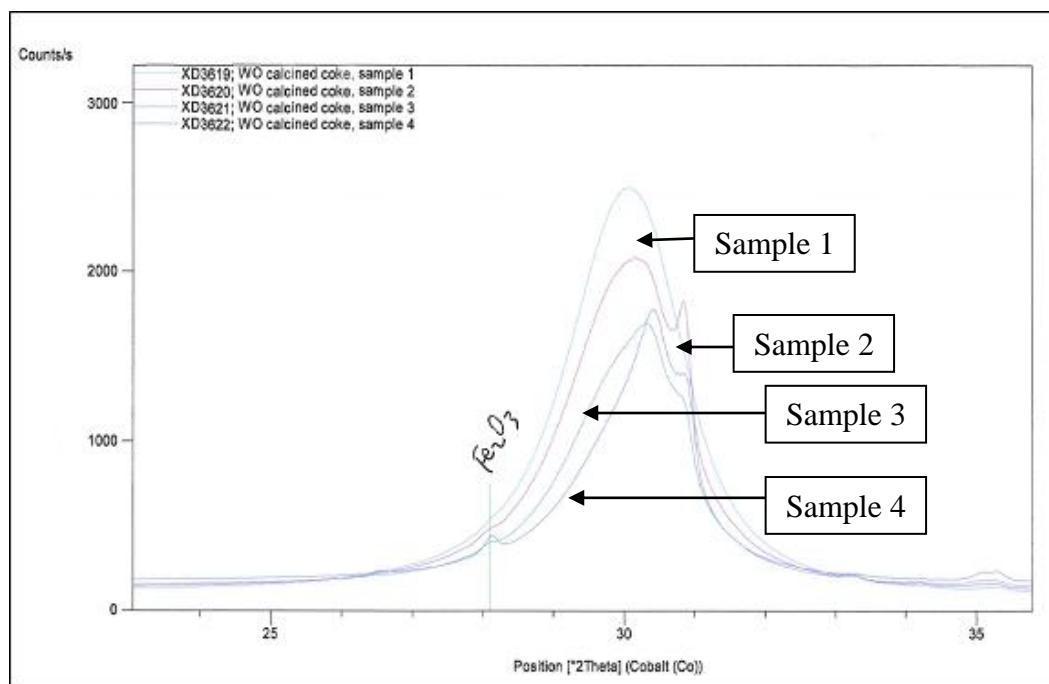


Figure 6-21 XRD trace showing graphite peaks between a 2θ angle of 25 and 35° in the Waxy Oil calcined cokes

The XRD trace of the four Waxy Oil calcined cokes presents broad peaks (within the graphite region) which are without doubt the product of overlapping individual peaks (as shown later in Figure 6-22).

Sample 1, with the lowest catalyst content, yields a broad Gaussian curve. As the catalyst content increases (Sample 2), the trace develops a small peak at a higher 2θ angle on the right shoulder. The XRD trace of Samples 3 and 4 indicates a broadening of the shoulder peak to the right of the trace.

As shown in Figure 6-15, the presence of elemental iron increases as the catalyst content increases. Both Ugarkorvic and Legin (1986) and Wang *et al.* (2001) have reported that an increase in the iron content of calcined petroleum coke lowers the temperature at which graphitisation occurs, presenting **two** overlapping peaks in the graphite region. Wang *et al.* (2001) identify these peaks as a thermal peak at a lower 2θ angle (depending on the original microstructural carbon anisotropy) and a peak at a higher 2θ angle due to catalytic “graphitisation”.

However, previous research by Wang *et al.* (1995) identified the presence of a third broad peak within the graphite region at a lower 2θ angle, ascribed to more disordered carbon. Baraniecki *et al.* (1969) refer to the development of multiple peaks in the graphite region as being a result of “multi-phase graphitisation”.

While the XRD trace of the Waxy Oil calcined cokes thus provides evidence of multi-phase graphitisation, the substantial overlapping of the 002 peaks warrants further investigation. In literature previously cited, Wang *et al.* (2001) used a narrow PSD for the iron additive (0.1-1.0 μm), which was equally dispersed within the carbon matrix. As the iron content increased, the microstructure trended towards a uniform mosaic microstructure.

In general terms, the increase in the catalyst concentration from Sample 1 to Sample 4 [as given by the chemical analysis (Table 6-3) and in the micrographs (Figure 8-11)] would support the development of the catalytically derived 002 peak.

The XRD trace of Waxy Oil calcined coke (Sample3) showing the three deconvoluted peaks named G1, G2 and G3 in the graphite region is shown in Figure 6-22. The interlayer spacings of the three peaks are shown in Table 6-4.

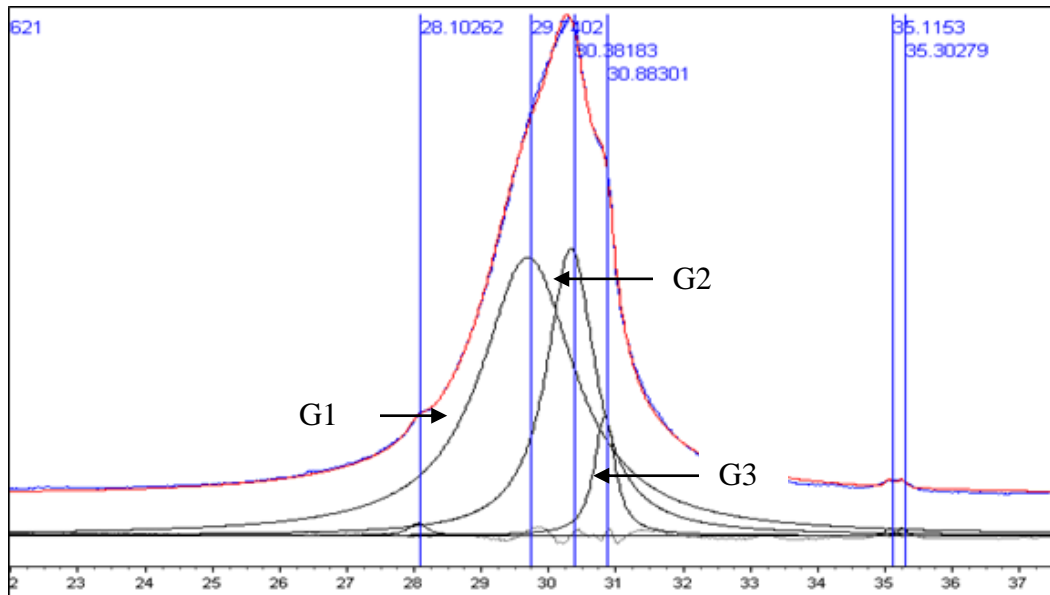


Figure 6-22 XRD trace showing graphite peaks G1, G2 and G3 in the Waxy Oil calcined coke

A description of the peaks to which random numbers G1, G2 and G3 were ascribed is given below:

- **G1:** This peak appears at a 2θ angle of 29.74° . As it appears at the lowest 2θ angle of the three peaks and is the broadest, it is thought to be associated with the least ordered carbon. As shown in Figure 6-13, mosaic microstructures are present in the immediate vicinity of the catalyst.
- **G2:** This peak appears at a 2θ angle of 30.38° . It is indicative of the improved development of the crystal structure, based on thermal treatment of the more anisotropic microstructures in the calcined coke.
- **G3:** This peak appears at a 2θ angle of 30.88° . As this peak is the sharpest, yielding the lowest d_{002} interlayer spacing, it is suggested that it is due to catalysed graphitisation (as a result of the iron content in the coke).

Table 6-4 Interlayer spacing of G1, G2 and G3 graphite peaks in Waxy Oil calcined cokes

Peak	Units	Sample 1	Sample 2	Sample 3	Sample 4
G1	Å	3.5040	3.4880	3.4850	3.4830
G2	Å	3.4410	3.4180	3.4140	3.4090
G3	Å	3.3760	3.3590	3.3600	3.3590

Å = 1×10^{-10} m

The ability of thermal treatment (in this case calcination) to increase the density of carbon depending on the microstructure of the coke is evident in the variation of the interlayer spacing of the G1 and G2 peaks. Although mosaic carbon microstructures (G1) are graphitisable, the microdomain boundaries limit the range within which crystal development occurs and thus present with higher interlayer spacings than G2 where there are fewer microdomain boundaries, allowing crystal development over a longer range.

The substantially lower interlayer spacing of the G3 002 peak is due to the mechanism of catalytic graphitisation which converts the carbon into quite highly ordered graphite, which is in agreement with the results of Wang *et al.* (1995).

Weismuller *et al.* (1995) suggest that carbon is catalytically transformed into highly ordered graphite by one of two mechanisms:

- Dissolution of carbon in the molten metal until super-saturation is reached, after which carbon precipitates in the form of crystalline graphite
- The formation of a metal carbide intermediate which decomposes to form crystalline graphite

As shown in Table 6-4, the interlayer spacing of the G1 and G2 peaks decreases slightly with increasing catalyst content. There is a substantial reduction of the interlayer spacing of G3 from Sample 1 to Sample 2, after which it remains constant for Samples 3 and 4.

While the degree of catalytic graphitisation is dependent on the concentration of iron (at least until the point of saturation) as reported by Wang *et al.* (2001) and Dhakate *et al.* (1997), it is the author's opinion that this may also be highly dependent on the PSD of the catalyst as smaller catalyst particles have a higher ratio of surface area to volume (compared with larger catalyst particles). Thus, with smaller catalyst particles the surface area contact with carbon in their direct vicinity is greater.

The interlayer spacing of the disordered (G1) and the thermal (G2) peaks in the graphite region decreases with an increasing catalyst content and a decrease in the overall anisotropy of the microstructure from Sample 1 to Sample 4. Although unexpected, this result is in agreement with that of Wang *et al.* (2001). This would suggest that the dominant graphitisation mechanism at 1 300 °C is catalytic.

6.5.4 Raman spectroscopy of Waxy Oil calcined coke

Raman spectroscopy was conducted on samples of Waxy Oil calcined coke in order to determine the influence of the catalyst content on the average ordering of the crystal structure. A detailed description of the experimental protocol is given in Chapter 5, Section 5.1.5.4.

Raman spectroscopy can distinguish between the various carbon phases and has been used to investigate the degree of crystallinity of carbonaceous materials (Sadezky *et al.*, 2005; Beyssac *et al.*, 2003). In the Raman spectrum both first- and second-order bands are observed in the region 200–4000 cm^{-1} . Five first-order bands have been identified and are designated the G, D1, D2, D3 and D4 bands (Sadezky *et al.*, 2005). The G band (1580 cm^{-1}) has E_{2g} symmetry as a result of the ideal graphitic lattice. It is therefore indicative of the degree of

graphitisation in the sample. The D bands are associated with disorder and defects present in the graphite layers (Sadezky *et al.*, 2005). The D1 (1350 cm^{-1} , A_{1g} symmetry) and D2 (1620 cm^{-1} , E_{2g} symmetry) bands indicate disorder in the graphene layers at the edges and on the surface layers respectively. The D3 band (1500 cm^{-1}) is indicative of the amount of amorphous carbon present in the sample, and the observation of the usually Raman inactive D4 band (1200 cm^{-1}) indicates disorder due to the presence of polyenes and ionic impurities.

Several ratios of the Raman bands have been proposed by Sadezky *et al.* (2005) and Beyssac *et al.* (2003) to give structural information regarding carbon samples. $R_1 = I_{D1}/I_G$ and $R_1' = I_{D2}/I_G$ are an indication of the relative disorder that exists within the graphene layers (Sadezky *et al.*, 2005), whereas $R_2 = I_{D1}/(I_{D1} + I_{D2} + I_G)$ gives information regarding the degree of organisation that exists in the sample (Beyssac *et al.*, 2003).

The Raman spectra of the four Waxy Oil calcined coke samples are shown in Figure 6-23 and the R_1 , R_1' and R_2 ratios in Table 6-5.

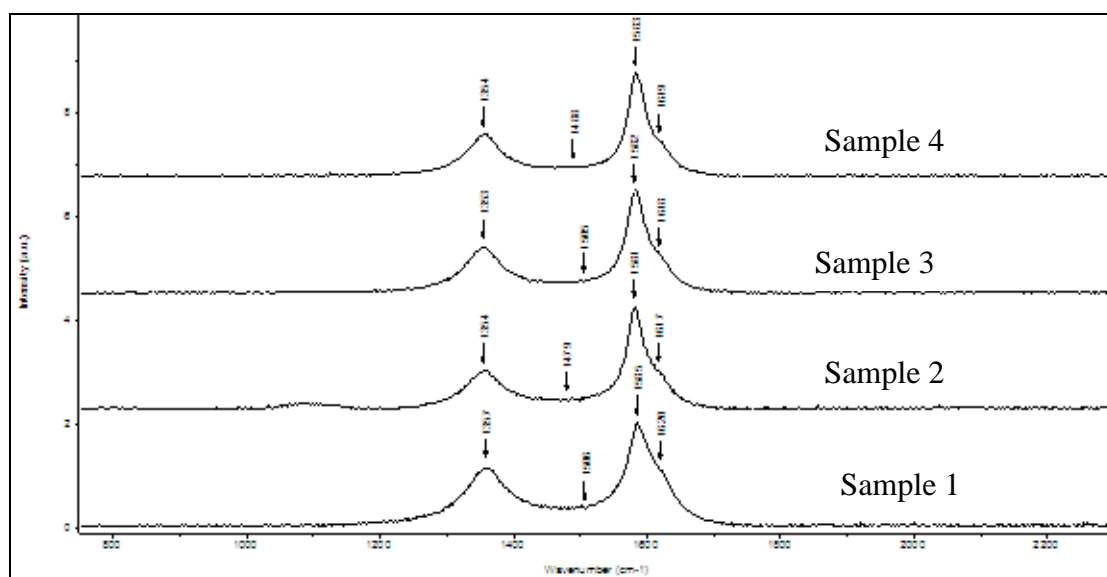


Figure 6-23 Raman spectra of Waxy Oil calcined cokes

Table 6-5 Comparative table of Raman spectra ratios (R_1 , R_1' and R_2) for Waxy Oil calcined cokes

Ratio	Calcined coke				References	
	Sample 1	Sample 2	Sample 3	Sample 4	Needle Coke	Graphite
R_1	0.624	0.357	0.452	0.400	0.769	0.062
R_1'	0.332	0.203	0.195	0.169	-	-
R_2	0.319	0.229	0.275	0.255	0.435	0.058

$$R_1 = I_{D1}/I_G$$

$$R_1' = I_{D2}/I_G$$

$$R_2 = I_{D1}/(I_{D1} + I_{D2} + I_G)$$

For the calcined needle coke no separate D2 band could be observed, but this does not mean that it has infinite graphitic domain, as the broad band at 1602 cm^{-1} probably represents both the G and D2 bands of calcined needle coke.

The calcined coke samples all have large R_1 values, but appear more ordered than the calcined needle coke. The R_1' ratio indicates that the crystallite width of the calcined cokes increases with increasing catalyst concentration. This is further evidence to support the dominance of catalytic graphitisation within the calcined cokes.

It is also interesting to note that the R_1 ratio of the calcined needle coke (Table 6-5; 0.769) is higher than that of any of the Waxy Oil calcined cokes. As the needle coke specification requires an ash content of less than 0.2%, the effect of catalytic graphitisation will be negligible and the crystal order will be determined by the development of the thermal graphite peak which, in turn, will depend on the microstructure. As the crystal development due to catalytic graphitisation will produce near-perfect graphite, the effect on the overall crystal structure will be both substantial and dominating.

6.6 Waxy Oil pre-graphite

Samples (1–4) of Waxy Oil green coke (> 2.0 mm, approximately 17 g) were thermally treated in a medium-frequency induction furnace to 2 000 °C with a soaking time of 5 min. Analyses conducted on the pre-graphites included real density, proximate analysis, XRD and Raman spectroscopy.

The proximate analysis of the pre-graphites is shown in Table 6-6.

Table 6-6 Analysis of Waxy Oil pre-graphites

	Units	Sample 1	Sample 2	Sample 3	Sample 4
VCM	mass%	0.6	0.8	0.6	0.4
Fixed carbon	mass%	97.5	95.2	93.0	88.4
Ash content	mass%	1.9	4.0	6.4	11.2

As the sample mass (approximately 17 g) for heat treatment (2 000 °C) of the Waxy Oil green coke was limited by the size of the graphite crucible, the ash content was estimated using TGA. The ash content of the pre-graphites is similar to that of the green coke and suggests that, even given the 82.0–84.6% yield, there was minimal iron sublimation.

6.6.1 Effect of catalyst content on the real density of Waxy Oil green and thermally treated cokes

The relationship between the catalyst concentration (Samples 1–4) and the corresponding real densities of the green and thermally treated cokes is shown in Table 6-7.

Table 6-7 Real density of Waxy Oil green coke, calcined coke and pre-graphite

	Units	Sample 1	Sample 2	Sample 3	Sample 4
Green coke	g.cm^{-3}	1.3879	1.4237	1.456	1.4792
Calcined coke	g.cm^{-3}	2.1024	2.1087	2.1124	2.1220
Pre-graphite	g.cm^{-3}	2.2113	2.1886	2.1774	2.1470

Increasing the catalyst content increases the real densities of the green and calcined coke. However, the real density of the pre-graphites decreases as a function of increasing catalyst concentration.

When proposing an explanation for these trends, it is necessary to consider both the yield and the effect of the phase of the iron-based catalyst in the green coke, calcined coke and pre-graphite.

The molecular weight of Fe_3O_4 (231.537) is considerably higher than that of carbon (12.011). As the bulk of the catalyst has a PSD below $75\ \mu\text{m}$ (the particle size used to determine the real density of the coke), its effect is likely to be included. This would thus explain the increase in the real density as the ash content of the green coke increased. With regard to the calcined coke, the yield as shown in Table 6-3 (86.5–90.6%) will increase the real density due to partial gasification of the carbon volatiles. However, as the calcination was conducted in nitrogen, it is suggested that the heavier components of the volatile carbon matter would carbonise to form solid carbon. As indicated in Figure 6-15, XRD data shows the presence of Fe_3O_4 , Fe_2O_3 and Fe. It is further suggested that the reduction of Fe_3O_4 would be only partial given the particle size range of the catalyst.

6.6.2 X-ray diffraction of Waxy Oil pre-graphite

XRD was conducted on samples of Waxy Oil pre-graphite in order to determine the influence of the catalyst concentration on the interlayer spacing of peaks in the graphite region. A detailed description of the experimental protocol is given in Chapter 5, Section 5.1.5.3.

6.6.2.1 Identification of peaks within the graphite region for Waxy Oil pre-graphites

An XRD trace of the graphite region of Waxy Oil pre-graphites is shown in Figure 6-24.

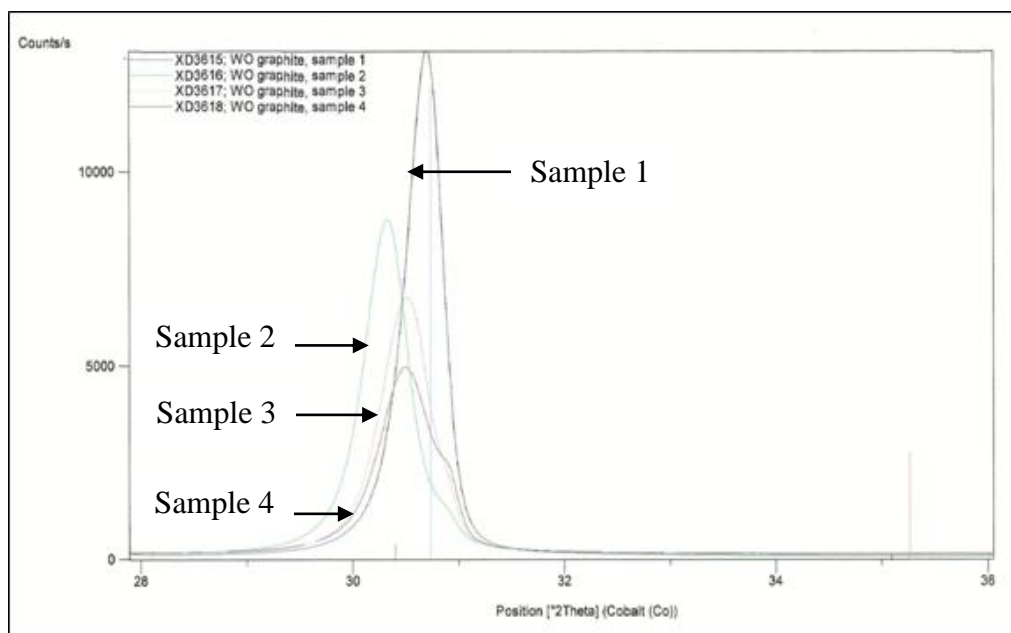


Figure 6-24 XRD trace showing peaks in the graphite region between a 2θ angle of 28 and 32° in the Waxy Oil pre-graphite

In comparison with the calcined coke (shown in Figure 6-21), the peaks in the graphite region of the Waxy Oil pre-graphites appear narrower and more intense. Sample 1 shows a narrow thermal peak. The peaks associated with Sample 2 to Sample 4 decrease in comparative (as the same amount of sample was used for the analysis) intensity and broaden while shifting to a higher 2θ angle.

There is a substantial difference in the 2θ angle of the thermal graphite peak between Sample 1 and Sample 2 of the pre-graphites. The shift towards a lower 2θ angle in the thermal graphite peak of Sample 2 indicates that Sample 1 shows a lower interlayer spacing. The apex of the thermal graphite peak for Samples 3 and 4 shifts to a higher 2θ angle (than Sample 1), which may indicate a co-dependence on both thermal and catalytic graphitisation mechanisms.

The XRD trace of Waxy Oil pre-graphites showing the three deconvoluted peaks in the graphite region identified as G1, G2 and G3 is shown in Figure 6-25.

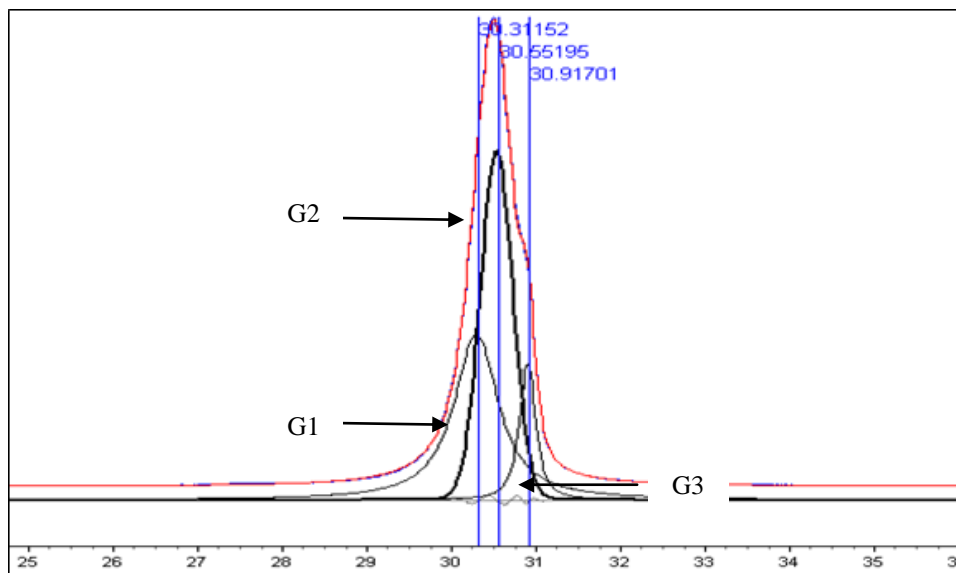


Figure 6-25 XRD trace showing graphite peaks G1, G2 and G3 in the Waxy Oil pre-graphites

For example, the three graphite peaks identified in Sample 1 calcined coke (G1, G2 and G3) are present in the Waxy Oil pre-graphites, but appear to have shifted to a higher 2θ angle. However, the 2 000 °C thermal treatment appears to narrow the width and increase the intensity of the thermal graphite peak (G2). This variation in the shape of the peaks as a result of thermal treatment is consistent with observations by Wang *et al.* (1995):

1. The disordered peak (G1) for calcined coke appears at a 2θ angle of 29.74° vs. the peak for pre-graphite which appears at a higher 2θ angle of 30.31° .
2. The thermal peak (G2) for calcined coke appears at a 2θ angle of 30.38° vs. the peak for pre-graphite which appears at a higher 2θ angle of 30.55° .
3. The catalytic peak (G3) for calcined coke appears at a 2θ angle of 30.88° vs. the peak for pre-graphite which appears at a higher 2θ angle of 30.92° .

The 2θ angle shifts for the disordered peak (G1; 0.57°) and the thermal peak (G2; 0.17°) are substantially greater than the shift for the catalytic peak (G3; 0.03°). This would indicate that

the thermal treatment (2 000 °C) had a more substantial effect on the development of the former peaks. Thus, in terms of the driving force for crystallographic development, it appears that thermal rather than catalytic graphitisation may be the driving force, especially in the pre-graphites where the catalyst concentration is lower. This is confirmed by studying the interlayer spacings associated with the peaks in the graphite region (G1, G2 and G3) shown in Table 6-8.

Table 6-8 Interlayer spacing of G1, G2 and G3 in the Waxy Oil pre-graphites

Peak	Units	Sample 1	Sample 2	Sample 3	Sample 4
G1	Å	3.348	3.429	3.417	3.422
G2	Å	3.360	3.404	3.390	-
G3	Å	3.355	3.357	3.354	3.357

$$\text{Å} = 1 \times 10^{-10} \text{ m}$$

The interlayer spacing of the G1 and G2 peaks are substantially lower in the pre-graphite coke than in the calcined coke, indicative of the effect of a temperature increase.

The increase in the interlayer spacing of Sample 1 to Samples 2 to 4 is caused partially by graphitisation due to thermal treatment and partially by catalytic graphitisation. As the catalyst concentration increases, the overall anisotropy of the carbon microstructure diminishes. Furthermore, when once the carbon immediately adjacent to the catalyst has been catalytically graphitised, it is not further graphitised by increasing thermal treatment; this is especially true in Samples 3 and 4.

The saturation of catalytic graphitisation for Samples 1 and 2 is thought to be due to the lower catalyst content. Both Mochida *et al.* (1980) and Wang *et al.* (2001) suggest that once carbon is catalytically graphitised, it is hardly graphitised further by the same catalyst even at a higher temperature.

6.6.3 Raman spectroscopy of Waxy Oil pre-graphite

The Raman spectrographic trace of the four Waxy Oil pre-graphites is shown in Figure 6-26. The intensities of the G, D1, D2, D3 and D4 peaks were used to determine the R_1 , R_1' and R_2 ratios shown in Table 6-9.

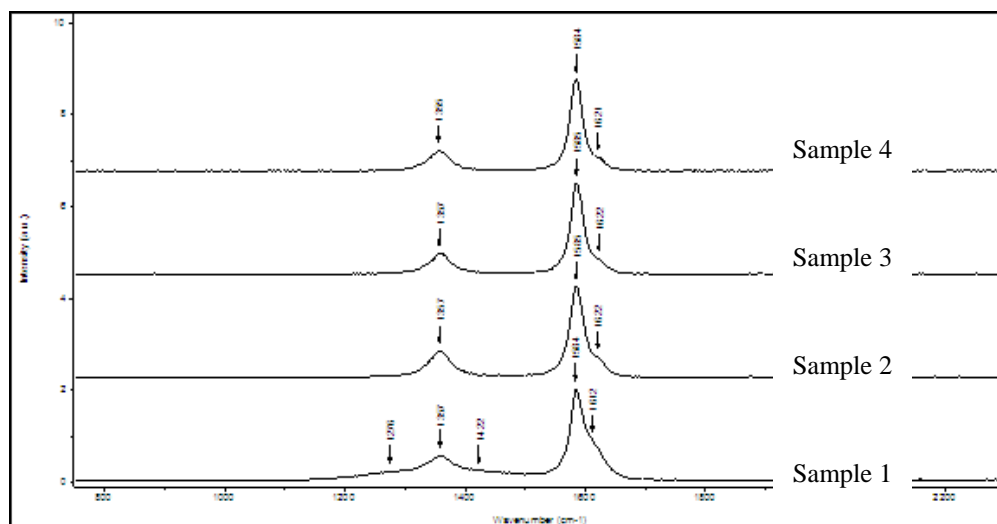


Figure 6-26 Raman spectra of Waxy Oil pre-graphites

Table 6-9 Comparison of Raman spectra ratios (R_1 , R_1' and R_2) for Waxy Oil pre-graphites

Ratio	Pre-graphites				References	
	Sample 1	Sample 2	Sample 3	Sample 4	Needle Coke	Graphite
R_1	0.206	0.284	0.225	0.225	0.769	0.062
R_1'	0.321	0.118	0.086	0.074	-	-
R_2	0.135	0.203	0.172	0.173	0.435	0.058

$$R_1 = ID1/IG$$

$$R_1' = ID2/IG$$

$$R_2 = ID1/(ID1 + ID2 + IG)$$

The pre-graphite samples have lower R_1 values (Table 6-9) than the calcined cokes (Table 6-5), showing that they have more ordered graphitic structures, which is expected as a result of thermal graphitisation, as indicated by the XRD data.

In comparison with the disordered and thermal peaks for the pre-graphite, the R_1 ratio (indicating the thickness of the crystallite) shows a similar trend between Samples 1 and 2, with Samples 3 and 4 being very much the same. The R_1' ratio indicates a decrease in the overall order as the catalyst content increases from Sample 1 to Sample 4. The increase in the order of pre-graphite Samples 3 and 4 compared with Sample 2 may indicate that saturation of catalytic graphitisation has not been reached.

6.7 Graphitisation of Waxy Oil green coke

This section examines the efficacy of catalyst sublimation from Waxy Oil green coke at a temperature of approximately 3 000 °C.

6.7.1 Analysis Waxy Oil green coke

Samples of Run of Coker (ROC)¹⁸ Waxy Oil green coke were obtained from the commercial delayed coker at Secunda, South Africa. After the green coke sample had been dried, it was sieved to produce the following particle size fractions:

- 0–1 mm
- 1–2 mm
- 2–4 mm
- 4–8 mm
- > 8 mm

A composite sample (2 200 g) composed of known masses of the size fractions was produced for the graphitisation experiment. The chemical analysis of the size fractions is shown in Table 6-10.

Table 6-10 Chemical analysis of Waxy Oil green coke particle size fractions

	Units	0–1 mm	1–2 mm	2–4 mm	4–8 mm	> 8 mm
Real density	g.cm ⁻³	1.4378	1.4564	1.4485	1.4774	1.4802
VCM	Mass%	10.79	12.23	12.01	12.34	9.82
Ash	Mass%	7.39	7.68	8.10	8.93	8.77
Iron (Fe)	Mass%	3.3467	3.5486	3.7163	3.8475	3.8419
Nickel (Ni)	Mass%	0.0001	0.0001	0.0001	0.0001	0.0001
Vanadium (V)	Mass%	0.0001	0.0001	0.0001	0.0001	0.0001
Calcium (Ca)	Mass%	0.1222	0.1158	0.1130	0.1094	0.1055
Silicon (Si)	Mass%	0.0386	0.0362	0.0035	0.0359	0.0380
Sodium (Na)	Mass%	0.0081	0.0044	0.0043	0.0047	0.0052

The VCM of the various size fractions ranges between 9.82 and 12.34%. Given the process of delayed coking, cutting and crushing, there is no specific evidence that VCM is in any way correlated to PSD variation.

The chemical analysis of Waxy Oil graphites is shown in Table 6-11.

Table 6-11 Chemical analysis of Waxy Oil graphite

	Units	0–1 mm	1–2 mm	2–4 mm	4–8 mm	> 8 mm
Carbon	Mass%	98.000	98.000	97.060	97.280	97.600
Hydrogen	Mass%	0.120	0.100	0.170	0.160	0.160
Nitrogen	Mass%	0.020	0.020	0.020	0.020	0.020
Sulphur	Mass%	0.003	0.003	0.002	0.004	0.011
Fixed carbon	Mass%	98.14	98.12	97.25	97.46	97.79
VCM	Mass%	0.03	0.01	0.14	0.17	0.14
Real density	g.cm ⁻³	2.2734	2.2722	2.2517	2.245	2.2597
CO ₂ reactivity	Mass%. 100 min ⁻¹	81.25	82.81	-	78.49	77.45
Air reactivity	Mass%	0.42	0.42	0.49	0.51	0.47

¹⁸ Run of Coker (ROC) refers to the full PSD of green coke after cutting and crushing and before any sieve screening.

	Units	0-1 mm	1-2 mm	2-4 mm	4-8 mm	> 8 mm
Resistivity	$\mu\Omega.m^{-1}$	324	307	298	318	323
Ash	Mass%	6.70	5.57	5.88	6.99	8.22
Iron (Fe)	Mass%	3.2310	2.9691	3.0762	3.3443	3.6012
Nickel (Ni)	Mass%	0.0001	0.0001	0.0001	0.0001	0.0001
Vanadium (V)	Mass%	0.0001	0.0001	0.0001	0.0001	0.0001
Calcium (Ca)	Mass%	0.0019	0.0019	0.0019	0.0018	0.0022
Silicon (Si)	Mass%	0.0585	0.0468	0.0509	0.0453	0.0507
Sodium (Na)	Mass%	0.0001	0.0010	0.0001	0.0001	0.0001
Total metals	Mass%	3.292	3.019	3.129	3.392	3.654

The percentile ash and iron loss vs. resistivity of Waxy Oil graphites is shown in Figure 6-27.

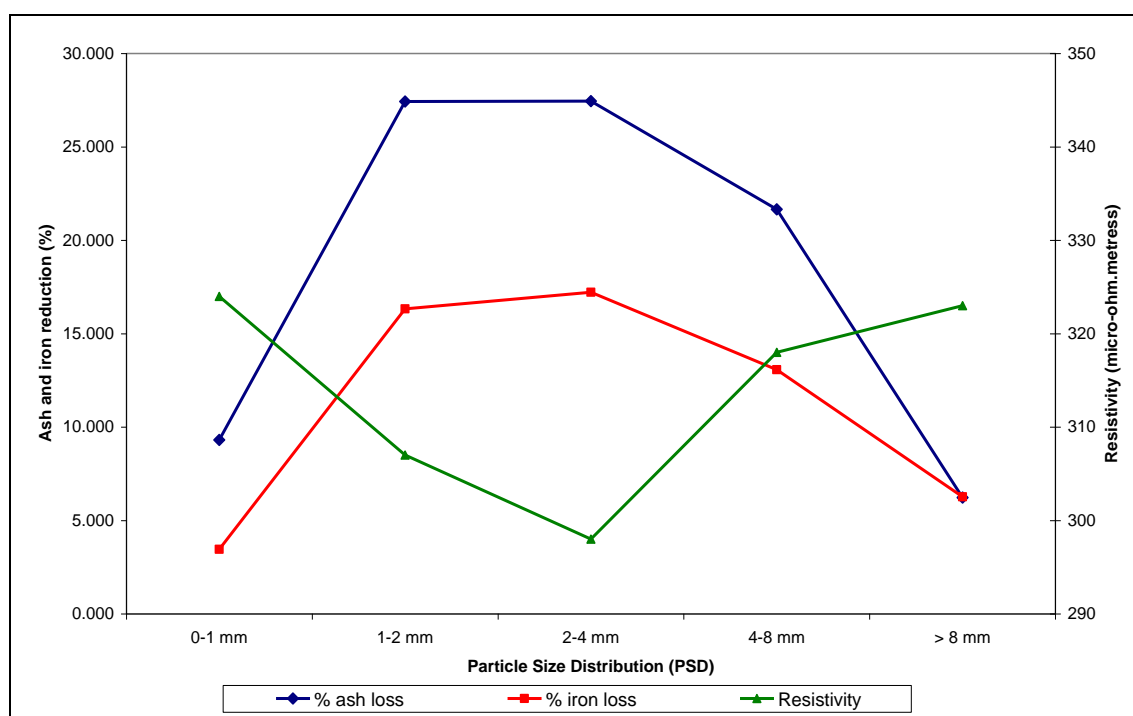


Figure 6-27 Graph showing the percentile loss of ash and iron from the green coke (during graphitisation) on the left axis vs. the resistivity of the graphite on the right axis

The ash reduction in Waxy Oil graphites is between 6 and 28%. The greatest percentile ash and iron loss occurs in the 1-2 mm and 2-4 mm particle size range with a reciprocal decrease in the resistivity. At both the ends of the particle size spectrum indicated (0-1 and > 8 mm) opposing forces of carbon surface area and catalyst exposure to the atmosphere may limit ash and iron reduction.

It was decided not to conduct further analysis on the Waxy Oil graphite samples (inclusive of optical microscopy, Raman spectroscopy and X-Ray diffraction) as it is evident from the results shown in Figure 6-7 that graphitisation would not be capable of removing the catalyst content to appropriate needle coke specification levels.

The discussion of the graphitisation section is limited due to the fact that it is the authors opinion that graphitisation was employed as a potential method to reduce the catalyst content. As it is clearly evident that this only occurred with a limited degree of success, further experimental analysis would not seem logical.

6.8 Conclusions – Influence of catalyst concentration on the characteristics of Waxy Oil coke

The current study presents data showing the effect of catalyst concentration (dominated by iron oxides) on the structural and reactivity profiles of commercial Waxy Oil green cokes, thermally treated to 1 400 °C (calcined cokes) and 2 000 °C (pre-graphites) .

The conclusions drawn from the current study of commercial Waxy Oil coke are:

- The real density of the green and calcined coke increases with increasing catalyst content due to the higher molecular weight of iron oxide compared with carbon. However, the contrary is true for the real densities of the pre-graphites, which decrease with increasing catalyst content due to reduction and partial sublimation of elemental iron.
- The oxidative consumption and carboxy reactivity is increased with increasing iron content as it acts as a promoter for both of these reactions.
- The catalyst obscures the formation of microstructural flow domains, acting predominantly as an inert barrier. As the catalyst size decreases, there is evidence of isotropic mosaic microstructures produced as iron oxide catalyses oxidative polymerisation.
- The reduction of iron oxide to elemental iron releases molecular oxygen which probably reacts with carbon to form carbon monoxide.
- The dominant crystal development mechanism during heat treatment of Waxy Oil coke to 1 300 °C is that of catalytic graphitisation, which is promoted by increasing iron content. However, further heat treatment of the Waxy Oil coke to 2 000 °C promotes a thermal graphitisation mechanism.
- Thermal treatment of Waxy Oil coke to 3 000 °C is not capable of reducing the ash content to needle coke specifications.

6.9 Recommendations – Influence of catalyst concentration on the characteristics of waxy oil coke

Based on the evidence provided in this chapter, a number of recommendations in respect of the production of needle coke from Waxy Oil can be made.

This option evaluates a process by which the catalyst is removed from Waxy Oil prior to carbonisation, followed by processes to decrease the catalytic oxidative polymerisation and the ash content.

It is further recommended that modification of the Waxy Oil be effected by means of a process called “sequential optimisation”. One or a combination of these processes will be employed to produce a modified carbonisation precursor in order to produce a more needle-like coke.

The recommended processes include:

1. Filtration of the Waxy Oil to remove the catalyst
2. Distillation of the filtered Waxy Oil
3. Thermal treatment of the filtered Waxy Oil
4. Thermal treatment and distillation of the filtered Waxy Oil

The modified Waxy Oils will be evaluated to determine the effect of the variation in chemical structure caused by the various processes. These results are discussed in Chapters 7 and 8.